Inorganic Chemistry

Article

pubs.acs.org/IC

Dinuclear Pyridine-4-thiolate-Bridged Rhodium and Iridium Complexes as Ditopic Building Blocks in Molecular Architecture

Montserrat Ferrer,*[,†] Daniel Gómez-Bautista,[‡] Albert Gutiérrez,[†] José R. Miranda,[‡] Guillermo Orduña-Marco,[‡] Luis A. Oro,[‡] Jesús J. Pérez-Torrente,*[,‡] Oriol Rossell,[†] Pilar García-Orduña,[‡] and Fernando J. Lahoz[‡]

[†]Departament de Química Inorgànica, Universitat de Barcelona, c/Martí i Franquès 1-11, 08028 Barcelona, Spain

[‡]Departamento de Química Inorgánica, Instituto de Síntesis Química y Catálisis Homogénea−ISQCH, Facultad de Ciencias, Universidad de Zaragoza−CSIC, C/Pedro Cerbuna 12, 50009 Zaragoza, Spain

Supporting Information

ABSTRACT: A series of dinuclear pyridine-4-thiolate (4-Spy)-bridged rhodium and iridium compounds $[M(\mu\text{-}4\text{-}Spy)(diolef)]_2$ [diolef = 1,5-cyclooctadiene (cod), M = Rh (**1**), Ir (**2**); diolef = 2,5-norbornadiene (nbd), M = Rh (**3**)] were prepared by the reaction of Li(4-Spy) with the appropriate compound $[M(\mu\text{-}Cl)(diolef)]_2$ (M = Rh, Ir). The dinuclear compound $[Rh(\mu\text{-}4\text{-}Spy)(CO)(PPh_3)]_2$ (**4**) was obtained by the reaction of $[Rh(acac)(CO)(PPh_3)]$ (acac = acetylacetonate) with 4-pySH. Compounds **1**−**4** were assessed as metalloligands in self-assembly reactions with the cis-blocked acceptors $[M(cod)(NCCH_3)_2](BF_4)$ [M = Rh (**a**), Ir (**b**)] and $[M(H_2O)_2(dppp)](OTf)_2$ [M = Pd (**c**), Pt (**d**); dppp = 1,3-bis(diphenylphosphino)propane]. The homometallic hexanuclear metallomacrocycles $[\{M_2(\mu\text{-}4\text{-}Spy)_2(cod)_2\}_2\{M(cod)\}_2](BF_4)_2$ (M = Rh $[(\mathbf{1a})_2]$, Ir $[(\mathbf{2b})_2]$) and the heterometallic hexanuclear metallomacrocycles $[\{Rh_2(\mu\text{-}4\text{-}Spy)_2(cod)_2\}_2\{Ir(cod)\}_2](BF_4)_2$ $[(\mathbf{1b})_2]$, $[\{Rh_2(\mu\text{-}4\text{-}Spy)_2(cod)_2\}_2\{M'(dppp)\}_2](OTf)_4$ (M′ = Pd $[(\mathbf{1c})_2]$, Pt $[(\mathbf{1d})_2]$), and $[\{Ir_2(\mu\text{-}4\text{-}Spy)_2(cod)_2\}_2\{M'(dppp)\}_2](OTf)_4$ (M′ = Pd $[(\mathbf{2c})_2]$, Pt $[(\mathbf{2d})_2]$) were obtained. NMR spectroscopy in combination with electrospray ionization mass spectrometry was used to elucidate the nature of the metalloligands and their respective supramolecular assemblies. Most of the synthesized species were found to be nonrigid in solution, and their fluxional behavior was studied by variable-temperature ^1H NMR spectroscopy. An X-ray diffraction study of the assemblies $(\mathbf{1a})_2$ and $(\mathbf{1d})_2$ revealed the formation of rectangular (9.6 Å × 6.6 Å) hexanuclear metallomacrocycles with alternating dinuclear (Rh_2) and mononuclear (Rh or Pt) corners. The hexanuclear core is supported by four pyridine-4-thiolate linkers, which are bonded through the thiolate moieties to the dinuclear rhodium units, exhibiting a bent-anti arrangement, and through the peripheral pyridinic nitrogen atoms to the mononuclear corners.

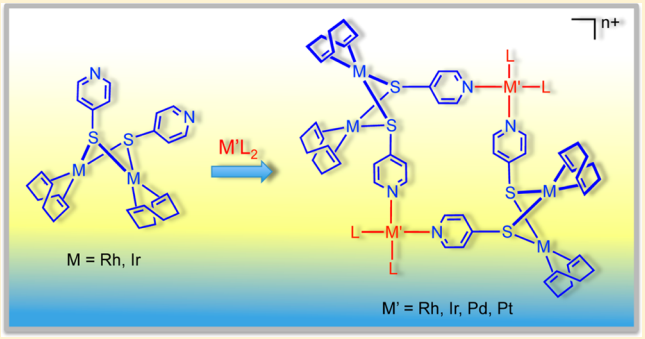

INTRODUCTION

The search for new and complex structures has been a motivating factor for the intensive study of metalla-supramolecular chemistry.[1−14] The sustained interest in this area is driven by the wide range of potential applications of these species in gas storage,[15,16] catalysis,[17−20] molecular magnetism,[21−23] optical materials,[24−26] sensing,[27−29] and many other areas.

In metal-based supramolecules, the metal units play an important role in controlling the structural geometries and tuning the chemical and physical properties of the compounds. In contrast with the synthesis of functionalized organic compounds, which can be achieved with high specificity by the use of well-defined reactions and reagents, the creation of complex metal-based molecules remains highly challenging because of the dynamic properties and lability of many coordination bonds. Although self-assembly has been proved to be a powerful tool for achieving a remarkable number of ordered structures,[11,12] such an approach depends largely on the availability of metal-based building blocks suitable for the assembly.

Lately we have become interested in the design and synthesis of heterometallic macrocyclic species[30−32] since the presence of different metal moieties can confer cooperative and/or dual behavior to the final species, particularly in relation with their participation in catalytic processes.[33−35] Although other methods have been described, the most common strategy to synthesize heterometallic macrocycles is modular self-assembly. This methodology requires the initial synthesis of metalloligands, that is, coordination complexes with strongly

Received: November 13, 2013
Published: January 17, 2014

   dx.doi.org/10.1021/ic402838y | *Inorg. Chem.* 2014, 53, 1699−1711

covalently bound ligands that have additional donor sites for coordination to other acceptor metallic building blocks.

In the general approach, monometallic building blocks are combined to yield self-assembled architectures. Despite the fact that the use of bimetallic units in combination with acceptor metallic complexes opens up new prospects for research in this area, only a handful number of bimetallic metalloligands have been described to date. In this context, Re_2,[36−38] Co_2,[39,40] and Mo_2[40,41] metal−metal-bonded entities bearing either two terminal pyridine or phosphine groups have been successfully employed for this purpose (Chart 1). Interestingly, the anionic

Chart 1. Schematic Representations of Reported Bimetallic Metalloligands

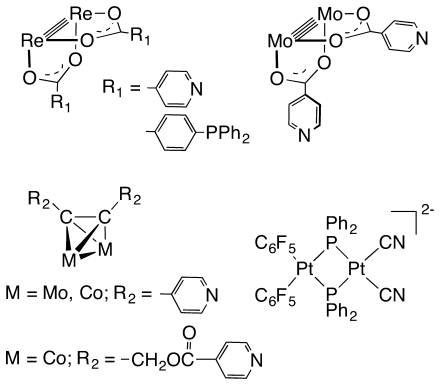

compound $[(C_6F_5)_2Pt(\mu\text{-}PPh_2)_2Pt(CN)_2]^{2-}$ described by Fornies and co-workers[42] is, to our knowledge, the unique example of a bimetallic building block lacking metal−metal bonds that coordinates to additional metal centers through the terminal cyanide groups that are coordinated to one of the platinum atoms of the binuclear complex (Chart 1).

In considering the goal of connecting dinuclear and mononuclear units, and given our experience in the synthesis and characterization of thiolate-bridged rhodium and iridium dinuclear complexes[43−47] and related hydrosulfide-bridged counterparts,[48] we envisaged the design of angular flexible dinuclear metalloligands of the type $[M(\mu\text{-}SR)L_2]_2$ (M = Rh, Ir) as precursors for new inorganic architectures by using adequately functionalized thiolato ligands. In this context, dinuclear d^8 transition-metal complexes with bridging thiolates have attracted widespread interest because of their electronic, structural, and conformational properties[45,49−55] and their catalytic activity in the hydroformylation of olefins under mild conditions.[56−60] Monodentate thiolato bridging ligands provide flexible structures that support a wide range of bonding and nonbonding metal distances by modification of the hinge angle between the rhodium coordination planes. In addition, the existence of several conformers arising from the relative disposition of the two thiolato ligands in the dinuclear framework and their possible interconversion confers to the complexes an unusual versatility from the point of view of their potential application as synthons in supramolecular chemistry.

On the other hand, pyridine-4-thiol (4-pySH) is a versatile ligand since it has the potential to coordinate to transition metals through either the sulfur atom or the nitrogen atom. Moreover, the deprotonated pyridine-4-thiolato (4-Spy) ligand usually coordinates to transition metals through the sulfur atom while leaving the pyridine moiety free. We thought that if the bimetallic complexes $[M(\mu\text{-}4\text{-}Spy)L_2]_2$ (M = Rh, Ir) based on pyridine-4-thiolato ligands could be prepared, the dangling pyridine groups would be available for further coordination to additional d^8 transition-metal centers such as those in the organometallic complexes $[M(cod)(CH_3CN)_2]^+$ (M = Rh, Ir; cod = 1,5-cyclooctadiene) or the dppp-chelated complexes $[M(H_2O)_2(dppp)]^{2+}$ [M = Pd, Pt; dppp = 1,3-bis(diphenylphosphino)propane] bearing labile acetonitrile and aqua ligands, respectively. Surprisingly, although the presence of uncoordinated pyridine groups strongly suggests the possibility of synthesizing novel supramolecular systems, the number of reported discrete metallomacrocycles incorporating this ligand is relatively small. In this regard, the trinuclear complexes $[Cp^*MCl(\mu\text{-}4\text{-}Spy)]_3$ (M = Ir,[61,62] Rh[62]) and $[PdCl(PPh_3)(\mu\text{-}4\text{-}Spy)]_3$,[63] the tetranuclear complex $[Cp^*Ir(4\text{-}Spy)(\mu\text{-}4\text{-}Spy)]_4$,[61] and the heterotetranuclear complex $[Pt(4,4'\text{-}dtbpy)(\mu\text{-}4\text{-}Spy)(ZnCl_2)]_2$ (dtbpy = 4,4′-di-*tert*-butyl-2,2′-bipyridine)[64] are, to the best of our knowledge, the only reported examples.

In this paper, we report on the synthesis of dinuclear rhodium or iridium organometallic ditopic metalloligands bridged by pyridine-4-thiolato ligands and their successful application in the construction of rectangular hexanuclear homo- and heterometallomacrocycles with alternating dinuclear (Rh_2 or Ir_2) and mononuclear (Rh, Ir, Pd, or Pt) corners.

EXPERIMENTAL SECTION

General Methods. All manipulations were performed under a dry argon or nitrogen atmosphere using Schlenk-tube techniques. Unless otherwise stated, reactions were carried out at room temperature. Liquid or solution transfers between reaction vessels were done via cannula. Solvents were dried by standard methods and distilled under argon or nitrogen immediately prior to use, or alternatively, a solvent purification system (Innovative Technologies) was used. NMR spectra were recorded at 250, 300, or 400 MHz with Varian or Bruker spectrometers at variable temperature. Chemical shifts are reported in parts per million and referenced to $SiMe_4$ using the signals of the deuterated solvent (^1H and ^{13}C) or to 85% H_3PO_4 as an external reference (^{31}P). Elemental C, H, and N analyses were performed in a PerkinElmer 2400 CHNS/O microanalyzer. Electrospray ionization mass spectrometry (ESI-MS) was performed on a Bruker MicroTof-Q mass spectrometer at the Universidad de Zaragoza or an LTQ-FT Ultra mass spectrometer (Thermo Scientific) at the Biomedical Research Institute (PCB-Universitat de Barcelona). MALDI-TOF mass spectra were obtained on a Bruker Miocroflex mass spectrometer using *trans*-2-[3-(4-*tert*-butylphenyl)-2-methyl-2-propenylidene]-malononitrile (DCTB) or dithranol (DIT) as a matrix.

Standard literature procedures were used to prepare the starting materials $[Rh(\mu\text{-}Cl)(diolef)]_2$ [diolef = cod,[65] norbornadiene (nbd)[66]], $[Ir(\mu\text{-}Cl)(cod)]_2$,[67] $[Rh(\mu\text{-}OMe)(cod)]_2$,[68] [Rh(acac)(CO)(PPh$_3$)] (acac = acetylacetonate),[69] $[Pd(H_2O)_2(dppp)](OTf)_2$ (**c**),[70] and $[Pt(H_2O)_2(dppp)](OTf)_2$ (**d**).[70] The cationic complexes $[M(diolef)(NCCH_3)_2]BF_4$ (diolef = cod, M = Rh (**a**), Ir (**b**); diolef = nbd, M = Rh) were obtained following a slight modification of the literature procedure.[71] 4-pySH was purchased from Aldrich, recrystallized from methanol/diethyl ether, and stored under nitrogen.

Synthesis of $[Rh(\mu\text{-}4\text{-}Spy)(cod)]_2$ (1). *Method A.* A solution of *n*-BuLi (0.6 mL, 0.942 mmol, 1.57 M in hexanes) was slowly added to a yellow suspension of 4-pySH (0.096 g, 0.864 mmol) in THF (5 mL) at 273 K, and the mixture was stirred for 1 h to give a white suspension of Li(4-Spy). Solid $[Rh(\mu\text{-}Cl)(cod)]_2$ (0.213 g, 0.432 mmol) was added to give an orange-brown suspension that was stirred for 4 h at room temperature. The solvent was removed under vacuum, and the residue was washed with cold methanol (2 × 3 mL) to give the compound as a brown solid that was filtered, washed with cold methanol, and dried under vacuum. Yield: 0.216 g (78%). *Method B.* 4-pySH (0.230 g, 2.069 mmol) was added to a solution of $[Rh(\mu\text{-}OMe)(cod)]_2$ (0.500 mg, 1.032 mmol) in dichloromethane (15 mL) to give an orange

dx.doi.org/10.1021/ic402838y | *Inorg. Chem.* 2014, 53, 1699−1711

solution that was stirred for 6 h. The solution was concentrated under vacuum to ca. 2 mL, and then diethyl ether (10 mL) was added to give a brown suspension. Further concentration and addition of diethyl ether gave the compound as a brown microcrystalline solid that was filtered, washed with diethyl ether (2 × 3 mL), and dried under vacuum. Yield: 0.556 g (84%). Anal. Calcd for $C_{26}H_{32}N_2Rh_2S_2$ (%): C, 49.22; H, 3.81; N, 4.41; S, 10.10. Found: C, 49.02; H, 4.01; N, 4.35; S, 10.25. ^{1}H NMR (CD_2Cl_2, 298 K, 300.13 MHz) δ: 8.26 (dd, 4H, J_{H-H} = 4.7 and 1.4 Hz, H_α), 7.28 (dd, 4H, J_{H-H} = 4.7 and 1.4 Hz, H_β) (4-Spy); 4.45 (br s, 8H, =CH), 2.46 (br, 8H, >CH_2), 2.01 (br, 8H, >CH_2) (cod). ^{13}C NMR ($CDCl_3$, 298 K, 74.46 MHz) δ: 150.0 (*CS*), 148.9, 128.8 (4-Spy); 81.5 (d, J_{C-Rh} = 11.7 Hz, =CH), 31.6 (>CH_2) (cod). MS (ESI+, CH_2Cl_2) *m*/*z*: 853 $[Rh_3(Spy)_2(cod)_3]^+$ (3%), 643 $[Rh_2(SpyH)(Spy)(cod)_2]^+$ (25%), 433 $[Rh(SpyH)_2(cod)]^+$ (100%), 322 $[Rh(SpyH)(cod)]^+$ (60%).

Synthesis of [Ir(μ-4-Spy)(cod)]$_2$ (2). $[Ir(\mu\text{-Cl})(cod)]_2$ (0.352 g, 0.524 mmol) and Li(4-Spy), formed in situ by the reaction of 4-pySH (0.117 g, 1.05 mmol) with *n*-BuLi (0.72 mL, 1.15 mmol, 1.6 M in hexanes), were reacted in THF (5 mL) for 10 h. The yellow suspension was concentrated under vacuum, and then methanol was added. The yellow solid was filtered, washed with methanol (3 × 4 mL), and dried under vacuum. Yield: 0.310 g (70%). Anal. Calcd for $C_{26}H_{32}N_2Ir_2S_2$ (%): C, 38.03; H, 3.93; N, 3.41; S, 7.81. Found: C, 38.15; H, 4.01; N, 3.36; S, 7.67. ^{1}H NMR (C_6D_6, 298 K, 400.16 MHz) δ: 8.27 (br d, 4H, J_{H-H} = 6.7 Hz, H_α), 6.99 (br d, 4H, J_{H-H} = 6.9 Hz, H_β) (4-Spy); 4.12 (br s, 8H, =CH), 2.01 (br, 8H, >CH_2), 1.52 (br, 8H, >CH_2) (cod). The ^{1}H NMR spectrum was obtained from a freshly prepared sample. On standing, the compound became insoluble in most of the usual organic solvents.

Synthesis of [Rh(μ-4-Spy)(nbd)]$_2$ (3). $[Rh(\mu\text{-Cl})(nbd)]_2$ (0.200 g, 0.434 mmol) and Li(4-Spy), formed in situ by the reaction of 4-pySH (0.096 g, 0.868 mmol) with *n*-BuLi (0.6 mL, 0.942 mmol, 1.57 M in hexanes), were reacted in THF (5 mL) for 15 min at 273 K to give a brown suspension that was stirred for 4 h. The solvent was removed under vacuum, and the residue was washed with cold methanol (2 × 3 mL) to give the compound as a brown solid that was filtered, washed with cold methanol, and dried under vacuum. Yield: 0.190 g (72%). Anal. Calcd for $C_{24}H_{24}N_2Rh_2S_2$ (%): C, 47.22; H, 3.96; N, 4.59; S, 10.50. Found: C, 47.13; H, 4.01; N, 4.52; S, 10.35. ^{1}H NMR ($CDCl_3$, 298 K, 400.16 MHz) δ: 8.31 (dd, 4H, J_{H-H} = 4.7 and 1.6 Hz, H_α), 6.97 (dd, 4H, J_{H-H} = 4.7 and 1.6 Hz, H_β) (4-Spy); 3.97 (s, 8H, =CH), 3.89 (s, 4H, CH), 1.36 (s, 4H, >CH_2) (nbd). MS (ESI+, CH_2Cl_2) *m*/*z*: 805 $[Rh_3(Spy)_2(nbd)_3]^+$ (15%), 611 $[Rh_2(SpyH)(Spy)(nbd)_2]^+$ (100%), 417 $[Rh(SpyH)_2(nbd)]^+$ (65%), 306 $[Rh(SpyH)(nbd)]^+$ (70%).

Synthesis of [Rh(μ-4-Spy)(CO)(PPh$_3$)]$_2$ (4). A solution of 4-pySH (0.045 g, 0.406 mmol) in CH_2Cl_2 (10 mL) was slowly added to a solution of $[Rh(acac)(CO)(PPh_3)]$ (0.200 g, 0.406 mmol) in CH_2Cl_2 (10 mL). The solution was stirred for 1 h to give a cloudy orange solution. The solvent was removed under vacuum, and the residue was extracted with a diethyl ether/CH_2Cl_2 (10:1) mixture (2 × 10 mL). The orange solution was filtered and concentrated under vacuum to ca. 1 mL. Slow addition of *n*-hexane (10 mL) and concentration gave a yellow solid. The precipitation was completed by the addition of *n*-hexane and further concentration under vacuum. The yellow-orange solid was filtered, washed with *n*-hexane, and dried under vacuum. Yield: 0.150 g (73%). Anal. Calcd for $C_{48}H_{38}N_2O_2P_2Rh_2S_2$ (%): C, 57.27; H, 3.80; N, 2.78; S, 6.37. Found: C, 57.26; H, 3.78; N, 2.66; S, 6.18. ^{1}H NMR ($CDCl_3$, 298 K, 300.13 MHz) δ: 8.39 (br s, 2H), 7.96 (br s, 2H), 7.85 (br s, 2H) (4-Spy); 7.56 (m, 12H), 7.38 (m, 6H), 7.28 (m, 12H) (Ph); 6.70 (br s, 2H, 4-Spy). ^{31}P{^{1}H} NMR ($CDCl_3$, 298 K, 121.48 MHz) δ: 38.26 (d, J_{P-Rh} = 157.9 Hz). MS (ESI+, CH_2Cl_2) *m*/*z*: 1007 $[Rh_2(SpyH)(Spy)(CO)_2(PPh_3)_2]^+$ (60%), 615 $[Rh(SpyH)_2(CO)(PPh_3)]^+$ (100%). IR (CH_2Cl_2) cm^{-1}: ν(CO), 1983 (s).

Synthesis of [{Rh$_2$(μ-4-Spy)$_2$(cod)$_2$}$_2${Rh(cod)}$_2$](BF$_4$)$_2$ [(1a)$_2$]. Solid $[Rh(cod)(NCCH_3)_2]BF_4$ (0.041 g, 0.109 mmol) was added to a suspension of $[Rh(\mu\text{-4-Spy})(cod)]_2$ (**1**) (0.070 g, 0.109 mmol) in THF (10 mL) to give an orange solution that was stirred for 2 h. Concentration of the solution to ca. 1 mL and slow addition of *n*-hexane (10 mL) gave the compound as a spongy orange solid that was filtered, washed with *n*-hexane (4 × 3 mL), and dried under vacuum. Yield: 0.064 g (62%). Anal. Calcd for $C_{68}H_{88}B_2F_8N_4Rh_6S_4$ (%): C, 43.43; H, 4.72; N, 2.98; S, 6.82. Found: C, 43.11; H, 4.90; N, 3.05; S, 6.90. ^{1}H NMR ($CDCl_3$, 298 K, 400.16 MHz) δ: 8.30 (d, 8H, J_{H-H} = 6.6 Hz, H_α), 7.20 (d, 8H, J_{H-H} = 6.6 Hz, H_β) (4-Spy); 4.79 (br s, 8H, =CH), 4.18 (br s, 8H, =CH), 3.97 (br s, 8H, =CH), 2.60 (br s, 16H, >CH_2), 2.36 (br s, 4H, >CH_2), 2.00 (br s, 4H, >CH_2), 1.98−1.86 (br s, 24H, >CH_2) (cod). ^{1}H NMR (CD_2Cl_2, 218 K, 300.13 MHz) δ: 8.12 (br s, 4H, H_α), 8.08 (br s, 4H, H_α), 7.52 (br s, 4H, H_β), 6.64 (br s, 4H, H_β) (4-Spy); 4.80 (br s, 4H, =CH), 4.68 (br s, 4H, =CH), 4.37 (br s, 4H, =CH), 3.93 (br s, 4H, =CH), 3.85 (br s, 8H, =CH), 2.47 (br s, 16H, >CH_2), 2.28 (br s, 8H, >CH_2), 2.10 (br s, 8H, >CH_2), 1.85 (br s, 16H, >CH_2) (cod). MS (ESI+, CH_2Cl_2) *m*/*z*: 1174 $[Rh_4(Spy)_3(cod)_4]^+$ (15%), 853 $[Rh_3(Spy)_2(cod)_3]^+$ (64%), 643 $[Rh_2(SpyH)(Spy)(cod)_2]^+$ (100%).

Synthesis of [{Ir$_2$(μ-4-Spy)$_2$(cod)$_2$}$_2${Ir(cod)}$_2$](BF$_4$)$_2$ [(2b)$_2$]. Solid $[Ir(cod)(NCCH_3)_2]BF_4$ (0.023 g, 0.049 mmol) was added to a yellow suspension of $[Ir(\mu\text{-4-Spy})(cod)]_2$ (**2**) (0.040 g, 0.049 mmol) in THF (10 mL), and the mixture was stirred overnight. The solvent was removed under vacuum, and the residue was washed with a CH_2Cl_2/diethyl ether (1:8) mixture (9 mL) to give a deep-red solid that was filtered, washed with diethyl ether (2 × 3 mL), and vacuum-dried. Yield: 0.055 g (93%). Anal. Calcd for $C_{68}H_{88}B_2F_8Ir_6N_4S_4$ (%): C, 33.79; H, 3.67; N, 2.32; S, 5.30. Found: C, 33.50; H, 3.51; N, 2.28; S, 5.25. ^{1}H NMR (CD_2Cl_2, 298 K, 400.16 MHz) δ: 8.28 (d, 8H, J_{H-H} = 5.2 Hz, H_α), 7.33 (m, 8H, H_β) (4-Spy); 4.57 (br s, 8H, =CH), 3.95 (br s, 8H, =CH), 3.79 (br s, 8H, =CH), 2.43 (m, 16H, >CH_2), 2.06 (m, 4H, >CH_2), 1.81 (m, 4H, >CH_2), 1.62 (m, 24H, >CH_2) (cod). MS (MALDI-TOF, DIT matrix, CH_2Cl_2) *m*/*z*: 1121 $[Ir_3(Spy)_2(cod)_3]^+$.

Synthesis of [{Rh$_2$(μ-4-Spy)$_2$(cod)$_2$}$_2${Ir(cod)}$_2$](BF$_4$)$_2$ [(1b)$_2$]. Solid $[Ir(cod)(NCCH_3)_2]BF_4$ (0.029 g, 0.062 mmol) was added to an orange suspension of $[Rh(\mu\text{-4-Spy})(cod)]_2$ (**1**) (0.040 g, 0.062 mmol) in CH_2Cl_2 (10 mL), and the mixture was stirred for 6 h. Workup as described above for (**1a**)$_2$ gave the compound as a red solid. Yield: 0.045 g (70%). Anal. Calcd for $C_{68}H_{88}B_2F_8Ir_2N_4Rh_4S_4$ (%): C, 39.66; H, 4.30; N, 2.72; S, 6.23. Found: C, 39.48; H, 4.02; N, 2.65; S, 6.08. ^{1}H NMR (CD_2Cl_2, 298 K, 400.16 MHz) δ: 8.27 (d, 4H, J_{H-H} = 5.6 Hz, H_α), 8.20 (d, 4H, J_{H-H} = 5.6 Hz, H_α), 7.20 (br s, 8H, H_β) (4-Spy); 4.77 (br s, 4H, =CH), 4.54 (br s, 4H, =CH) (Rh-cod); 4.27 (br s, 8H, =CH), 4.00 (br s, 8H, =CH) (Rh-cod and Ir-cod); 2.59 (m, 12H, >CH_2), 2.48 (m, 16H, >CH_2), 1.97 (m, 12H, >CH_2), 1.55 (m, 8H, >CH_2) (cod). MS (MALDI-TOF, DIT matrix, CH_2Cl_2) *m*/*z*: 943 $[Rh_2Ir(Spy)_2(cod)_3]^+$.

Synthesis of [{Rh$_2$(μ-4-Spy)$_2$(cod)$_2$}$_2${Pd(dppp)}$_2$](OTf)$_4$ [(1c)$_2$]. Solid $[Pd(H_2O)_2(dppp)](OTf)_2$ (0.027 g, 0.030 mmol) was added to a CH_2Cl_2 solution (5 mL) of $[Rh(\mu\text{-4-Spy})(cod)]_2$ (**1**) (0.020 g, 0.030 mmol). After 2 h of stirring, the reaction mixture was filtered, concentrated to 5 mL under vacuum, and precipitated with *n*-hexane. A yellow solid was obtained. Yield: 0.035 g (78%). Anal. Calcd for $C_{110}H_{116}N_4Pd_2P_4Rh_4O_{12}F_{12}S_8$ (%): C, 45.26; H, 4.01; N, 1.92; S, 8.79. Found: C, 45.43; H, 3.98; N, 1.95; S, 8.70. ^{1}H NMR ($CDCl_3$, 298 K, 250.13 MHz) δ: 8.33 (br s, 8H, H_α) (4-Spy); 7.57 (m, 16H), 7.32 (m, 24H) (Ph); 6.74 (d, 8H, J_{H-H} = 5.0 Hz, H_β) (4-Spy); 4.67 (br s, 8H, =CH), 3.98 (br s, 8H, =CH) (cod); 3.15 (m, 8H, P−CH_2−C) (dppp); 2.56 (br s, 8H, >CH_2), 2.36 (br s, 8H, >CH_2) (cod); 2.10 (m, 20H) (>CH_2 cod + C−CH_2−C dppp). ^{31}P{^{1}H} NMR ($CDCl_3$, 298 K, 101.25 MHz) δ: 6.5 (s). HRMS (ESI+, acetone) *m*/*z*: 1311.1 $[\{Rh_2(Spy)_2(cod)_2\}_2\{Pd(dppp)\}_2(OTf)_2]^{2+}$ (90%), 823.7 $[\{Rh_2(Spy)_2(cod)_2\}_2\{Pd(dppp)\}_2(OTf)]^{3+}$ (8%).

Synthesis of [{Rh$_2$(μ-4-Spy)$_2$(cod)$_2$}$_2${Pt(dppp)}$_2$](OTf)$_4$ [(1d)$_2$]. Solid $[Pt(H_2O)_2(dppp)](OTf)_2$ (0.029 g, 0.030 mmol) was added to a CH_2Cl_2 solution (5 mL) of $[Rh(\mu\text{-4-Spy})(cod)]_2$ (**1**) (0.020 g, 0.030 mmol), and the mixture was stirred for 2 h. Workup as described above for (**1c**)$_2$ gave the compound as an orange solid. Yield: 0.039 g (80%). Anal. Calcd for $C_{110}H_{116}N_4Pt_2P_4Rh_4O_{12}F_{12}S_8$: C, 42.67; H, 3.78; N, 1.81; S, 8.28. Found: C, 42.81; H, 3.81; N, 1.76; S, 8.19. ^{1}H NMR (CD_2Cl_2, 298 K, 500.13 MHz) δ: 8.28 (d, 8H, J_{H-H} = 5.0 Hz, H_α) (4-Spy); 7.59 (m, 16H), 7.35 (m, 24H) (Ph); 6.78 (d, 8H, J_{H-H} = 5.0 Hz, H_β) (4-Spy); 4.65 (br s, 8H, =CH), 4.05 (br s, 8H, =CH)

dx.doi.org/10.1021/ic402838y | *Inorg. Chem.* 2014, 53, 1699−1711

(cod); 3.21 (m, 8H, P−CH_2−C) (dppp); 2.54 (m, 8H, >CH_2), 2.40 (br s, 8H, >CH_2) (cod); 2.14 (m, 12H) (>CH_2 cod + C−CH_2−C dppp); 2.03 (m, 8H, >CH_2) (cod). $^{31}P\{^1H\}$ NMR ($CDCl_3$, 298 K, 101.25 MHz) δ: −14.5 (s, J_{P-Pt} = 2989 Hz). HRMS (ESI+, acetone) m/z: 1399.1 $[\{Rh_2(Spy)_2(cod)_2\}_2\{Pt(dppp)\}_2(OTf)_2]^{2+}$ (100%), 882.7 $[\{Rh_2(Spy)_2(cod)_2\}_2\{Pd(dppp)\}_2(OTf)]^{3+}$ (30%).

Synthesis of $[\{Ir_2(\mu\text{-4-Spy})_2(cod)_2\}_2\{Pd(dppp)\}_2](OTf)_4$ [(2c)$_2$]. Solid $[Pd(H_2O)_2(dppp)](OTf)_2$ (0.026 g, 0.030 mmol) was added to a CH_2Cl_2 suspension (5 mL) of $[Ir(\mu\text{-4-Spy})(cod)]_2$ (**2**) (0.025 g, 0.030 mmol), and the mixture was stirred for 2 h. Workup as described above for (**1c**)$_2$ gave the compound as an orange solid. Yield: 0.037 g (75%). Anal. Calcd for $C_{110}H_{116}N_4Pd_2P_4Ir_4O_{12}F_{12}S_8$ (%): C, 40.33; H, 3.57; N, 1.71; S, 7.83. Found: C, 40.57; H, 3.54; N, 1.70; S, 7.90. ^1H NMR ($CDCl_3$, 298 K, 250.13 MHz) δ: 8.46 (br s, 8H, H_α) (4-Spy); 7.67 (m, 16H), 7.32 (m, 24H) (Ph); 6.78 (br s, 8H, H_β) (4-Spy); 4.41 (br s, 8H, =CH), 3.65 (br s, 8H, =CH) (cod); 3.16 (br s, 8H, P−CH_2−C) (dppp); 2.80−1.90 (m, 36H) (>CH_2 cod + C−CH_2−C dppp). $^{31}P\{^1H\}$ NMR ($CDCl_3$, 298 K, 101.25 MHz) δ: 6.5 (s). HRMS (ESI+, acetone) m/z: 3127.2 $[\{Ir_2(Spy)_2(cod)_2\}_2\{Pd(dppp)\}_2(OTf)_3]^+$ (1%); 1489.2 $[\{Ir_2(Spy)_2(cod)_2\}_2\{Pd(dppp)\}_2(OTf)_2]^{2+}$ (100%); 943.1 $[\{Ir_2(Spy)_2(cod)_2\}_2\{Pd(dppp)\}_2(OTf)]^{3+}$ (5%).

Synthesis of $[\{Ir_2(\mu\text{-4-Spy})_2(cod)_2\}_2\{Pt(dppp)\}_2](OTf)_4$ [(2d)$_2$]. Solid $[Pt(H_2O)_2(dppp)](OTf)_2$ (0.023 g, 0.020 mmol) was added to a CH_2Cl_2 suspension (5 mL) of $[Ir(\mu\text{-4-Spy})(cod)]_2$ (**2**) (0.020 g, 0.020 mmol), and the mixture was stirred for 2 h. Workup as described above for (**1c**)$_2$ gave the compound as a red solid. Yield: 0.029 mg (70%). Anal. Calcd for $C_{110}H_{116}N_4Pt_2P_4Ir_4O_{12}F_{12}S_8$: C, 38.26; H, 3.38; N, 1.62; S, 7.43. Found: C, 37.95; H, 3.34; N, 1.68; S, 7.50. ^1H NMR ($CDCl_3$, 298 K, 250.13 MHz) δ: 8.50 (d, 8H, J_{H-H} = 2.5 Hz, H_α) (4-Spy); 7.68−7.34 (m, 40H) (Ph); 6.83 (d, 8H, J_{H-H} = 5.0 Hz, H_β) (4-Spy); 4.41 (br, 8H, =CH), 3.68 (m, 8H, =CH) (cod); 3.27 (m, 8H, P−CH_2−C) (dppp); 2.43 (br, 16H, >CH_2) (cod); 2.01 (br m, 20H) (>CH_2 cod + C−CH_2−C dppp). $^{31}P\{^1H\}$ NMR ($CDCl_3$, 298 K, 101.25 MHz) δ: −14.9 (s, J_{P-Pt} = 3054 Hz). HRMS (ESI+, acetone) m/z: 3303.4 $[\{Ir_2(Spy)_2(cod)_2\}_2\{Pd(dppp)\}_2(OTf)_3]^+$ (1%); 1577.7 $[\{Ir_2(Spy)_2(cod)_2\}_2\{Pd(dppp)\}_2(OTf)_2]^{2+}$ (50%); 1002.1 $[\{Ir_2(Spy)_2(cod)_2\}_2\{Pd(dppp)\}_2(OTf)]^{3+}$ (15%).

Crystal Structure Determination of (1a)$_2$ and (1d)$_2$. Data for (**1a**)$_2$ were collected at 150(1) K using a Bruker SMART APEXII CCD diffractometer at station 9.8 of the SRS Daresbury Laboratory. Radiation was monochromatized with a silicon (111) crystal (λ = 0.69340 Å). X-ray diffraction data for (**1d**)$_2$ were collected at 100(2) K with graphite-monochromatized Mo Kα radiation (λ = 0.71073 Å) on a Bruker SMART APEX CCD diffractometer. In both cases, ω narrow rotation (0.3°) scans were used, and the measured intensities were integrated and corrected for the absorption effect with the programs SAINT-PLUS[72] and SADABS.[73] Structures were solved by direct methods with SHELXS-97.[74,75] Refinement was carried out by full-matrix least-squares on F^2 for all data with SHELXL-97.[76] All hydrogen atoms were calculated and refined using a riding model. The PARST program[77,78] was used in the geometrical analysis of the complexes.

Although several crystals were tested, in all cases the data for (**1a**)$_2$ showed broad reflections with generally low intensity, most probably because of quick loss of solvent for these samples. The eventual data collected prevented a proper conventional least-squares refinement but allowed the appropriate identification of the metallocyclic skeleton of the molecule. Similar situations have been described for other related macromolecular complexes where big cavities contain very labile and/or disordered solvent molecules.[79−83] The limited quality of the crystal data for (**1a**)$_2$ did not allow a conventional refinement of all non-hydrogen atoms including anisotropic thermal parameters (ADPs). The atoms of the counterions (found to be disordered) were refined with isotropic thermal parameters, and a common thermal parameter was used for the fluorine atoms; geometrical restraints for both the B−F bond lengths and F−B−F angles were also applied. Moreover, some additional restraints in ADPs were defined for some bonds of cod ligands to ensure fulfillment of the Hirshfeld test. Finally, one of the pyridine rings was found to be disordered; atoms of this group were included in the model in two sets of positions and isotropically refined with complementary occupancy factors [0.59/0.41(2)] including geometrical restraints.

In the final steps of both structural refinements, clear evidence of the existence of large solvent-accessible voids and the presence of highly disordered solvent was observed. All attempts to model these molecules were unsuccessful. An analysis of the solvent region was therefore performed using the SQUEEZE program.[84] The contribution of the estimated solvent content to the total structure factors was calculated and incorporated in further least-squares refinements. A summary of the crystal data and structure refinement parameters is reported in Table 1.

Table 1. Crystal Data and Structure Refinement

	(1a)$_2$	(1d)$_2$
molecular formula	$C_{69}H_{90}N_4Rh_6S_4\cdot 2BF_4\cdot CH_2Cl_2\cdot 1.25C_6H_{14}$	$C_{106}H_{116}N_4P_4Pt_2Rh_4S_4\cdot 4CF_3O_3S\cdot 4CH_2Cl_2\cdot 7C_4H_{10}O$
formula weight	2073.39	3954.79
T (K)	150	100
λ (Å)	0.6934	0.73071
crystal system	monoclinic	monoclinic
space group	$C2/c$	$P2_1/n$
a (Å)	39.803(4)	14.4510(9)
b (Å)	16.5686(16)	18.3763(11)
c (Å)	28.098(3)	27.5849(17)
β (deg)	115.516(2)	90.8530(10)
V (Å^3)	16723(3)	7324.5(8)
Z	8	2
μ (mm^{-1})	1.174	2.729
D_{calc} (g/cm^3)	1.647	1.793
F(000)	8356	3988
crystal dimensions (mm)	0.01 × 0.03 × 0.08	0.05 × 0.07 × 0.08
T_{min}/T_{max}	0.627/1	0.598/0.746
collected/unique reflections	50004/11966	47211/16801
R_{int}	0.1101	0.0458
data/restraints/parameters	11966/188/783	16801/2/755
R_1 $[I > 2\sigma(I)]^a$	0.1028	0.0480
wR_2 (all data)^b	0.3229	0.1336

$^aR_1 = \sum||F_o| - |F_c||/\sum|F_o|$. $^bwR_2 = \{[\sum w(F_o^2 - F_c^2)^2]/[\sum w(F_o^2)^2]\}^{1/2}$

RESULTS AND DISCUSSION

Synthesis of the Dinuclear Rhodium and Iridium Ditopic Metalloligands $[M(\mu\text{-4-Spy})(diolef)]_2$. The synthesis of bimetallic metalloligands containing pyridine-4-thiolato ligands was readily accomplished following two procedures described in the literature by our group. The first one[43] makes use of the lithium salt Li(4-Spy), which was prepared in situ by reaction of 4-pySH with *n*-BuLi in THF (method A). As shown in Scheme 1, the reaction of Li(4-Spy) with the compounds $[M(\mu\text{-Cl})(cod)]_2$ in a 2:1 molar ratio led to the formation of the thiolate-bridged complexes $[M(\mu\text{-4-Spy})(cod)]_2$ [M = Rh (**1**), Ir (**2**)], which were isolated as air-sensitive orange-brown (**1**) and yellow-brown (**2**) solids in good yields. While compound **1** is soluble in most of the common organic solvents, the iridium derivative **2** shows limited solubility in all of them. Compound **1** was obtained in similar yield by an alternative method[45] involving direct protonation of the methoxide bridging ligands in the complex $[Rh(\mu\text{-OMe})(cod)]_2$ by 4-pySH in dichloromethane (method B).

The binuclear compounds **1** and **2** were characterized by elemental analysis, mass spectrometry (ESI+), and NMR

dx.doi.org/10.1021/ic402838y | Inorg. Chem. 2014, 53, 1699−1711

Scheme 1. Preparation of Dinuclear Thiolate-Bridged Rhodium and Iridium Metalloligands

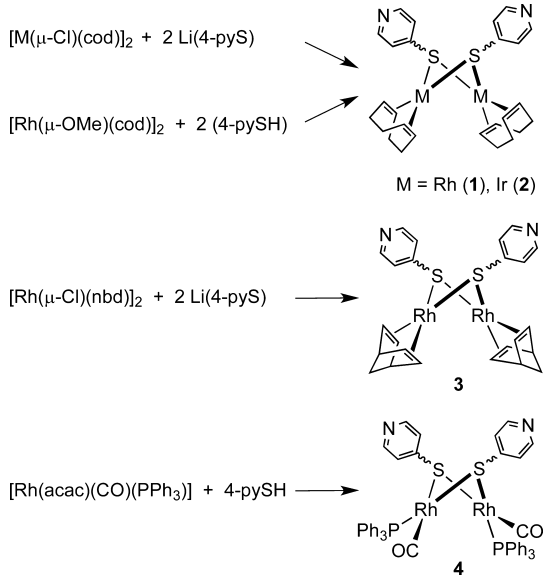

spectroscopy. The MS (ESI+) spectrum of **1** in CH_2Cl_2 displayed a peak at m/z 643 corresponding to the dinuclear protonated species $[Rh_2(SpyH)(Spy)(cod)_2]^+$ that supports the formation of the desired compound. In spite of numerous attempts [ESI(+), FAB(+), and MALDI-TOF in different solvents], mass spectrometry did not provide confirmation of the nuclearity of compound **2**. However, satisfactory mass spectra were obtained when the dinuclear iridium compound was a constituent of the supramolecular assemblies that will be described later on.

The room-temperature ^{1}H NMR spectra of both **1** and freshly prepared **2** (in CD_2Cl_2 and C_6D_6, respectively) showed the expected signals for the α and β protons of the pyridine rings as well as those attributable to the =CH and $>CH_2$ protons of the 1,5-cyclooctadiene ligand, which were observed as a set of broad resonances. The =CH protons were observed as single resonances at 4.45 and 4.12 ppm for **1** and **2**, respectively. The two resonances at 2.46 and 2.01 for **1** and 2.01 and 1.52 for **2** were assigned to the nonequivalent protons within each of the $>CH_2$ groups (exo and endo protons). The straightforward pattern is indicative of the high symmetry of the obtained species. This simplicity could be also found in the $^{13}C\{^1H\}$ NMR spectrum of **1** (the spectrum of **2** could not be registered because of its low solubility), where apart from the three resonances assigned to the pyridine carbons, only one doublet for the olefinic =CH groups (81.5 ppm, J_{C-Rh} = 11.7 Hz) and a single resonance for the $>CH_2$ carbons (31.6 ppm) were observed for the 1,5-cyclooctadiene ligands. The features of the ^{1}H NMR spectrum suggest a fluxional behavior derived from an open-book structure resulting from the μ-(1:2-κ^2S) coordination mode of the two pyridine-4-thiolato ligands with a syn disposition. In fact, inversion of the nonplanar Rh_2S_2 ring accounts for the equivalence of all the olefinic =CH protons and carbons at room temperature.[43,45,85−87] Interestingly, a number of thiolate-bridged dinuclear rhodium and iridium complexes containing cyclooctadiene ligands display a syn-endo conformation in the solid state and exhibit dynamic behavior similar to that found for complex **1**.[45,86−89] Unfortunately, the ^{1}H NMR spectrum was not resolved even at 193 K, which points to a low-energy ring inversion process.

A dirhodium compound analogous to **1** but containing 2,5-norbornadiene ligands was also synthesized. $[Rh(\mu\text{-Spy})(nbd)]_2$ (**3**) was obtained from $[Rh(\mu\text{-Cl})(nbd)]_2$ and Li(4-Spy) as a brown solid in good yield (Scheme 1). Its characterization by elemental analysis, NMR spectroscopy, and mass spectrometry confirmed its analogy with compound **1**. In fact, its ^{1}H NMR spectrum also evidenced a fluxional behavior that renders equivalent the =CH and CH protons of the two nbd ligands.

Treatment of the mononuclear complex $[Rh(acac)(CO)(PPh_3)]$ with 1 equiv of 4-pySH in dichloromethane gave a deep-orange solution from which the dinuclear compound $[Rh(\mu\text{-4-Spy})(CO)(PPh_3)]_2$ (**4**) was isolated as a yellow-orange solid in good yield. Complex **4** was characterized by elemental analysis, mass spectrometry, and IR and NMR spectroscopies. The dinuclear formulation of compound **4** relies on the ESI+ mass spectrum, which showed a peak at m/z 1007 corresponding to the protonated molecular cation $[Rh_2(SpyH)(Spy)(CO)_2(PPh_3)_2]^+$.

The ^{1}H NMR spectrum of **4** in $CDCl_3$ also featured broad resonances, although in this case the pyridine-4-thiolato ligands were not equivalent and showed four resonances at 8.39, 7.96, 7.85, and 6.70 ppm. The $^{31}P\{^1H\}$ NMR spectrum was in accordance with the equivalence of the two triphenylphosphine ligands because only a doublet due to the coupling with the rhodium nucleus was observed ($^1J_{P-Rh}$ = 158 Hz). The inequivalence of the bridging ligands suggests a dinuclear structure with a cis disposition of the bulky triphenylphosphine ligands. Most probably, the thiolato ligands display an anti conformation with the endo substituent at the side of the molecule with the small carbonyl ligands, as is usually found in related complexes.[45]

General Strategy for Self-Assembly Reactions. Once prepared and fully characterized, the bimetallic metalloligands described above were used to design self-assembled metallomacrocycles. The thiolate-bridged dinuclear compounds feature two peripheral pyridine nitrogen donor atoms that are available for coordination to suitable metal fragments. However, in view of the lack of conformational rigidity of this family of compounds, different possibilities of self-assembly could be envisaged depending on the relative disposition of the pyridine rings (Figure 1). This feature provides highly flexible linkages for the design of supramolecular assemblies.

While the syn-exo isomer could yield discrete metallomacrocycles as a result of its combination with metal building blocks having two available coordination sites at 180°, acceptor units having two coordination positions at 90° should be necessary in order to get a discrete assembly in the case of the syn-endo isomer, which displays an almost linear orientation of the pyridine fragments. The anti isomer, however, has the possibility of forming discrete species either by combination with 90° or 180° acidic metal fragments. Nevertheless, it has to be considered that the disposition of the donor moieties in these metalloligands does not rule out the formation of self-assembled polymeric species such as infinite chains or networks.

Although the choice of a metal-containing acceptor with an adequate angle between the vacant positions may be decisive for the control of the reactivity at the metal site, the nature of the final products will depend on their thermodynamic stabilities, since it is known that self-assembly is a

dx.doi.org/10.1021/ic402838y | Inorg. Chem. 2014, 53, 1699−1711

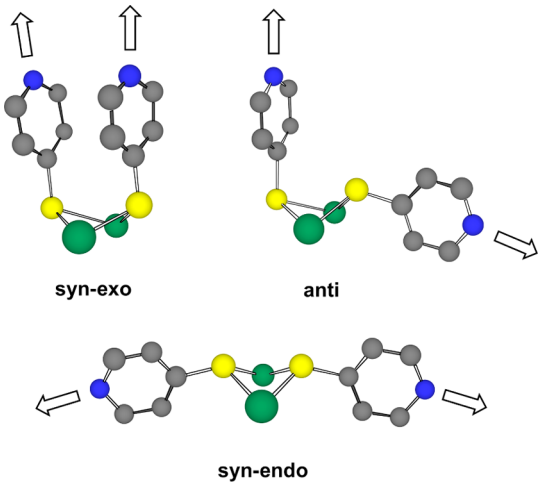

Figure 1. Different isomers arising from the relative disposition of the pyridine rings in the thiolate-bridged dinuclear metalloligands.

thermodynamically controlled process. As we have pointed out above, we chose two different types of acceptor building blocks, namely, $[M(diolef)(CH_3CN)_2]^+$ (diolef = cod; M = Rh, Ir) and $[M(H_2O)_2(dppp)]^{2+}$ (M = Pd, Pt), where two adjacent coordination positions are blocked by bidentate ligands in order to ensure an angle of 90° between the acidic sites.

Self-Assembly Reactions Involving $[M(\mu\text{-Spy})(cod)]_2$ [M = Rh (1), Ir (2)] Metalloligands and $[M(diolef)(CH_3CN)_2]^+$ [diolef = cod, nbd; M = Rh (a), Ir (b)] Acceptor Units. The bimetallic pyridine-4-thiolate-bridged compounds $[M(\mu\text{-Spy})(cod)]_2$ [M = Rh (**1**), Ir (**2**)] were found to undergo self-assembly with both of the solvent-stabilized species $[M(cod)(NCCH_3)_2]^+$ [M = Rh (**a**), Ir (**b**)] in dichloromethane at room temperature to give exclusively the rectangular hexanuclear metallomacrocycles $(\mathbf{1a})_2$, $(\mathbf{1b})_2$, and $(\mathbf{2b})_2$, as shown in Scheme 2. After completion of the reactions [2 h for $(\mathbf{1a})_2$ and $(\mathbf{1b})_2$ and 12 h for $(\mathbf{2b})_2$], the species were obtained as solids in moderate to good yields (60−90%) and characterized by elemental analysis, mass spectrometry (ESI+ or MALDI), and NMR spectroscopy. In addition, single crystals of compound $(\mathbf{1a})_2$ were grown by slow diffusion of hexane into a dichloromethane solution of the complex at 258 K and were further characterized by X-ray diffraction analysis.

A molecular representation of the cation of $(\mathbf{1a})_2$ is depicted in Figure 2, and selected structural parameters are summarized in Table 2. The rhodium atoms of both bimetallic $[Rh(\mu\text{-4-SPy})(cod)]_2$ fragments display a slightly distorted square-planar geometry resulting from the coordination of sulfur atoms of two pyridine-4-thiolato ligands and a cod molecule chelated through the two olefinic bonds. Similar acute S−Rh−S angles [in the range 79.49(17)−80.68(15)°] and trans angles S−Rh−G (where G is the centroid of an olefinic C═C bond) close to 180° [167.4(6)−177.0(6)°] are observed. The rhodium atoms are slightly displaced out of their coordination mean plane [Rh(1), 0.111(1); Rh(2), 0.074(1); Rh(3), 0.008(2); Rh(4), 0.114(2) Å], evidencing the distortion from an ideal square-planar conformation, as previously observed in related thiolate-bridged Rh(I) complexes.[47] The central Rh_2S_2 cores are folded, as indicated by the hinge angles between the two rhodium coordination planes [78.1(2) and 75.4(3)° for the Rh(1)−S(2)−Rh(2)−S(4) and Rh(3)−S(1)−Rh(4)−S(3) bimetallic fragments, respectively]. Long intermetallic distances of 2.924(3) and 2.965(3) Å are found, excluding metal−metal

Scheme 2. Self-Assembly of Hexanuclear Rhodium and Iridium Metallomacrocycles

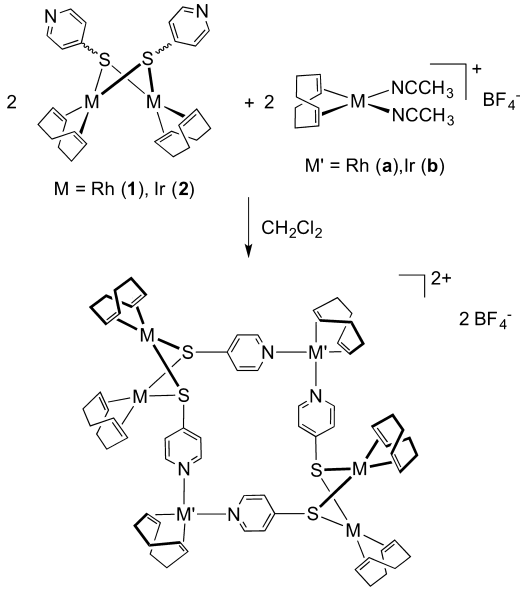

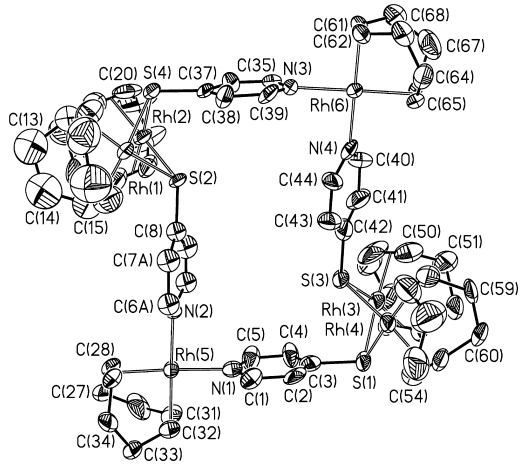

Figure 2. Molecular structure of the cation of $(\mathbf{1a})_2$ drawn at the 40% probability level. For clarity, hydrogen atoms and the minor component of the disordered pyridine ring have been omitted.

interactions. Both the dihedral angles and interatomic distances nicely agree with values reported for the related compounds $[Rh(\mu\text{-2,3,5,6-tetrafluoro-4-(trifluoromethyl)benzenethiolato})(cod)]_2$ [73.85° and 2.9595(3) Å],[90] $[\{Rh(cod)\}_2(\mu\text{-}S,S\text{-EtSNS})]OTf$ [EtSNS = $EtNC(S)Ph_2P{=}NPPh_2C(S)NEt$] (77.56° and 2.942 Å),[91] and $[Rh(\mu_2\text{-methylthiolato})(cod)]_2$ (75.86° and 2.947 Å).[89]

The bimetallic metalloligands with a bent (anti) arrangement coordinate to the Rh(cod) fragments, giving rise to hexanuclear metallomacrocycles exhibiting an unusual alternating disposition of bi- and monometallic corners. The anti disposition of the thiolato ligands in the dinuclear rhodium corners contrasts with the syn disposition observed in the parent dinuclear thiolate-bridged building block (see above). As the syn−anti

dx.doi.org/10.1021/ic402838y | Inorg. Chem. 2014, 53, 1699−1711

Table 2. Selected Bond Lengths and Angles for $(1a)_2$[a]

bond	length (Å)	angle	size (deg)	angle	size (deg)
Rh(1)−S(2)	2.380(5)	S(2)−Rh(1)−S(4)	80.68(15)	S(1)−Rh(3)−S(3)	79.49(17)
Rh(1)−S(4)	2.366(5)	S(2)−Rh(1)−G(1)	167.4(6)	S(1)−Rh(3)−G(7)	176.6(7)
Rh(2)−S(2)	2.387(5)	S(2)−Rh(1)−G(2)	101.7(7)	S(1)−Rh(3)−G(8)	92.7(7)
Rh(2)−S(4)	2.366(4)	S(4)−Rh(1)−G(1)	88.7(5)	S(3)−Rh(3)−G(7)	102.0(9)
Rh(3)−S(1)	2.377(6)	S(4)−Rh(1)−G(2)	174.8(6)	S(3)−Rh(3)−G(8)	172.0(8)
Rh(3)−S(3)	2.384(5)	G(1)−Rh(1)−G(2)	88.3(8)	G(7)−Rh(3)−G(8)	85.9(11)
Rh(4)−S(1)	2.383(5)	S(2)−Rh(2)−S(4)	80.55(15)	S(1)−Rh(4)−S(3)	79.71(15)
Rh(4)−S(3)	2.366(5)	S(2)−Rh(2)−G(3)	101.1(5)	S(1)−Rh(4)−G(9)	92.9(8)
Rh(5)−N(1)	2.105(13)	S(2)−Rh(2)−G(4)	170.1(5)	S(1)−Rh(4)−G(10)	167.6(7)
Rh(5)−N(2)	2.151(10)	S(4)−Rh(2)−G(3)	177.0(6)	S(3)−Rh(4)−G(9)	172.6(6)
Rh(6)−N(3)	2.094(12)	S(4)−Rh(2)−G(4)	91.1(6)	S(3)−Rh(4)−G(10)	98.9(6)
Rh(6)−N(4)	2.047(13)	G(3)−Rh(2)−G(4)	86.9(8)	G(9)−Rh(4)−G(10)	88.5(9)
mean Rh−G	2.017(6)	N(1)−Rh(5)−N(2)	88.4(4)	N(3)−Rh(6)−N(4)	88.3(4)
		N(1)−Rh(5)−G(5)	177.2(5)	N(3)−Rh(6)−G(11)	178.0(5)
		N(1)−Rh(5)−G(6)	90.6(6)	N(3)−Rh(6)−G(12)	91.9(5)
		N(2)−Rh(5)−G(5)	93.5(5)	N(4)−Rh(6)−G(11)	91.8(6)
		N(2)−Rh(5)−G(6)	176.8(6)	N(4)−Rh(6)−G(12)	178.1(6)
		G(5)−Rh(5)−G(6)	87.6(7)	G(11)−Rh(6)−G(12)	88.1(6)

[a] G(n) represents the centroid of the nth olefinic bond among the cod ligands.

interconversion cannot be explained by inversion of the nonplanar Rh_2S_2 ring, the formation of the metallomacrocycles should involve a sulfur inversion. This can occur either by breaking of a Rh−S bond (dissociative mechanism) or through a planar transition state in which the S atom is sp^2-hybridized (nondissociative mechanism).[52]

The Rh(5) and Rh(6) metal centers at the mononuclear corners also display square-planar coordination that is less distorted than for the metal atoms of the bimetallic fragments [out-of-plane distances of 0.008(1) and 0.001(2) Å for Rh(5) and Rh(6), respectively]. The N(1)−Rh(5)−N(2) and N(3)−Rh(6)−N(4) angles, which are very close to 90°, generate a rectangular molecule core whose dimensions can be roughly estimated from the Rh(5)···S(1)···Rh(6)···S(4) distances as 6.641(3) Å × 9.613(4) Å (Figure 3). The mean plane of the metallomacrocycle, defined by Rh(5), Rh(6), sulfur, and nitrogen atoms, is almost parallel to the bc crystallographic plane.

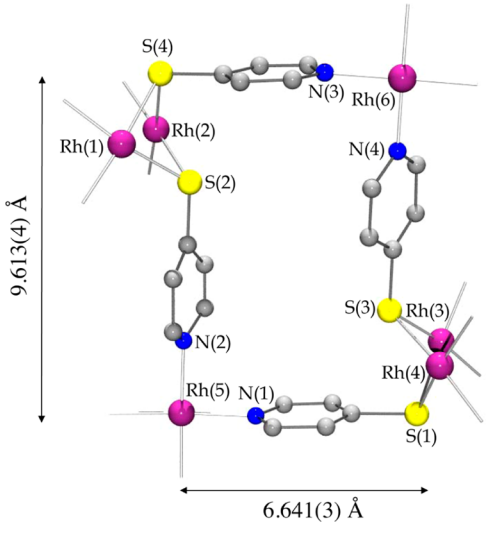

Figure 3. Schematic view of the rectangular molecular core of $(1a)_2$.

The conformational geometry, with pyridine-4-thiolato ligands as intermetallic linkers, causes the rhodium atoms of the bimetallic fragments to be placed above and below this mean plane, with the bulkiest cod ligands being located in the outer part of the metallomacrocycle. Apparently, no steric impediment seems to hinder the accessibility to the metallomacrocyclic cavity. Along the a axis, the structure shows the presence of pairs of molecules with the metallomacrocycles in a parallel disposition but twisted 90° with respect to each other (Figure 4). The minimal distances between Rh atoms within a pair and between pairs are 7.668(2) and 7.212(2) Å, respectively.

Interestingly, the coordination chemistry of the complexes $[M(\mu\text{-4-Spy})(cod)]_2$ that results in the formation of the macrocyclic species contrasts with that of the related dinuclear thiophenolato (SPh)-bridged complexes $[M(\mu\text{-SPh})(cod)]_2$ (M = Rh, Ir). The latter reacted with solvent-stabilized cationic $[M(cod)L_2]^+$ fragments to give cationic trinuclear aggregates $[M_3(\mu\text{-SPh})_2(cod)_3]^+$ that are formed by a triangular arrangement of metal atoms capped on each side by two triply bridging phenylthio ligands.[43] These species showed outstanding stability, and in fact, related trinuclear ions corresponding to halves of the self-assembled species were observed in the mass spectra of the three macrocyclic compounds $(1a)_2$, $(1b)_2$, and $(2b)_2$, namely, $[Rh_3(Spy)_2(cod)_3]^+$ (m/z 853), $[Rh_2Ir(Spy)_2(cod)_3]^+$ (m/z 943) and $[Ir_3(Spy)_2(cod)_3]^+$ (m/z 1221), respectively.

On the other hand, the room-temperature ^{1}H NMR spectra of the obtained compounds (Figures S1−S6 in the Supporting Information) were in agreement with the existence of a single species that undergoes a dynamic process in solution. Indeed, the metallomacrocycles $[\{M_2(\mu\text{-4-Spy})_2(cod)_2\}_2\{M'(cod)\}_2]^{2+}$ (M = M′= Rh $[(1a)_2]$; M = Rh, M′ = Ir $[(1b)_2]$; M = M′ = Ir $[(2b)_2]$) are fluxional as evidenced by a variable-temperature (VT) NMR study. The ^{1}H NMR spectrum of $(1a)_2$ at 218 K (Figure 5 bottom) is in agreement with the C_{2h} symmetry of the structure found in the solid state. Thus, the two sets of resonances at 8.12/6.64 and 8.08/7.52 ppm correspond to the two types of 4-Spy ligands in the metallomacrocycle having exo and endo dispositions in the dinuclear rhodium subunit. The

dx.doi.org/10.1021/ic402838y | Inorg. Chem. 2014, 53, 1699−1711

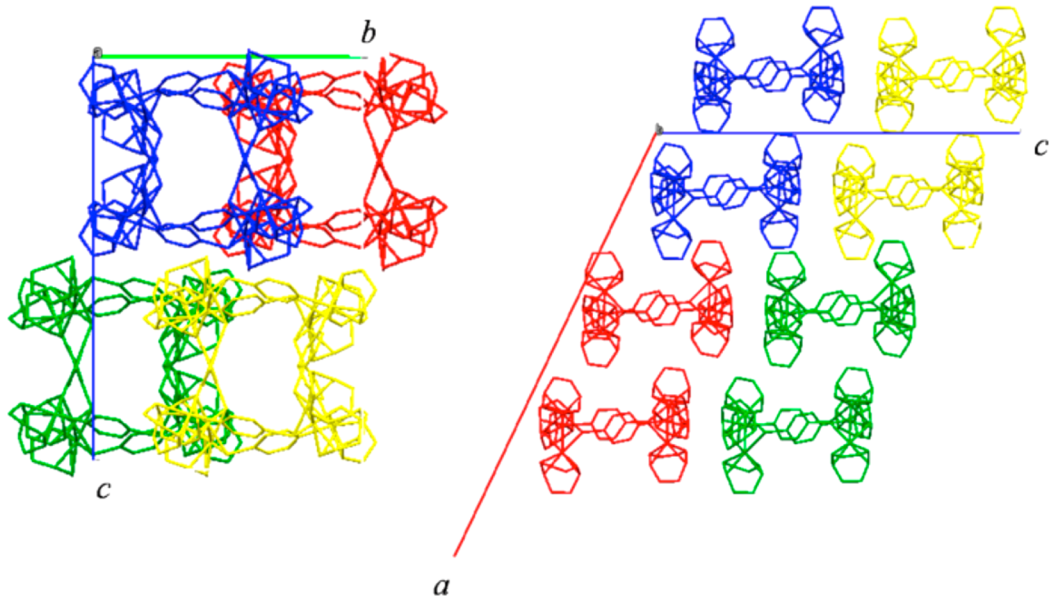

Figure 4. Molecular packing of $(\mathbf{1a})_2$ along the crystallographic *a* and *b* axes. To properly show the cavity, counterions and solvent have been omitted. Different colors are used to identify pairs of molecules with overlapping metallomacrocycles.

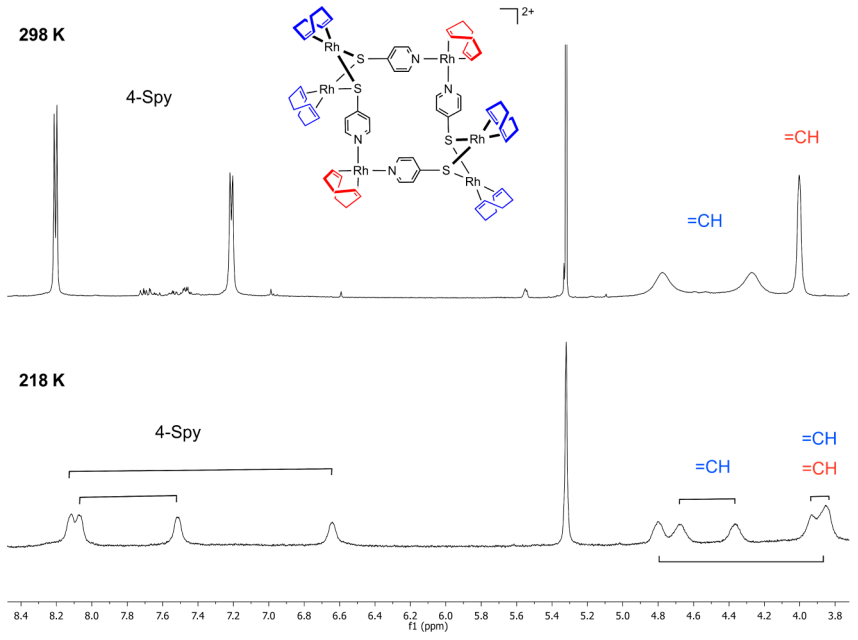

Figure 5. Low-field region of the ^{1}H NMR spectra (CD_2Cl_2) of metallomacrocycle $(\mathbf{1a})_2$ at 298 K (top) and 218 K (bottom).

olefinic protons of the cod ligands show five resonances, one of them with double the intensity of the others, which were unambiguously identified by means of the ^{1}H−^{1}H COSY spectrum at 218 K (Figure S5 in the Supporting Information). Thus, the expected four resonances for the two olefinic bonds of the cod ligands in the dinuclear subunit were observed at 4.80/3.85 and 4.68/4.37 ppm. In addition, the signals at 3.93 and 3.85 ppm, which showed no coupling, correspond to the cod ligands of the Rh(cod) units bonded to the pyridine fragments.

In contrast, the spectrum at 298 K (Figure 5 top) is deceptively simple and shows equivalent 4-Spy ligands and only three resonances (8H each) for the =CH protons of the cod ligands. The ^{1}H−^{1}H NOESY spectrum (Figure S6 in the Supporting Information) was particularly informative because it allowed the identification of the =CH resonances of the cod ligand in the dinuclear subunit at 4.79 and 4.18 ppm through the observation of proximity cross-peaks with the signal at 7.20 ppm that corresponds to the β protons of the 4-Spy ligands. In addition, exchange cross-peaks between the two =CH resonances were observed, which indicates that the fluxional process makes the two protons of the same olefinic bond equivalent. This process also renders equivalent the olefinic protons of the cod ligands in the Rh(cod) units bonded to pyridine, which were observed at 3.97 ppm.

As has been pointed out above, inversion of the nonplanar Rh_2S_2 ring in dinuclear complexes having thiolato ligands as bridges is a common phenomenon that is responsible for their fluxional behavior. In this case, this process would account for the pattern of resonances observed at room temperature.

dx.doi.org/10.1021/ic402838y | *Inorg. Chem.* 2014, 53, 1699−1711

However, the ring-flipping process results not only in the exchange of the thiolato ligands with exo and endo disposition but also in the movement of the bulky cod ligands toward the inner part of the metallomacrocycle. Thus, this process requires the concerted motion of the metallomacrocycle in order to allow the rotation about the C−S bonds just for relocating the cod ligands in the outside part of the metallomacrocycle. For that reason, breaking of the Rh−N bonds in order to assist this process should not be ruled out. Interestingly then, the existence of an equilibrium between the supramolecular species and their corresponding building blocks seems to be responsible for this dynamic behavior.

The ^{1}H NMR spectrum of the compound $[\{Ir_2(\mu\text{-}4\text{-}Spy)_2(cod)_2\}_2\{Ir(cod)\}_2]^{2+}$ $[(\mathbf{2b})_2]$ at room temperature is very similar to that described for the $[Rh_6]$ species, which suggests a similar fluxional behavior for this compound. However, in this case the fluxional process could not be frozen at low temperature, precluding further investigation.

The synthesis of metallomacrocycles containing different diolefin ligands, as for example $[\{Rh_2(\mu\text{-}4\text{-}Spy)_2(cod)_2\}_2\{Rh(nbd)\}_2]^{2+}$, was unsuccessful. Thus, even though the reaction of $[Rh(\mu\text{-}4\text{-}Spy)(cod)]_2$ (**1**) with the metal fragment $[Rh(nbd)(NCCH_3)_2]^+$ resulted in the formation of $[Rh_6]$ metallomacrocycles, the self-assembly took place in a nonselective way because at least four different species were observed in the aromatic region of the ^{1}H NMR spectrum, probably as a consequence of scrambling of metal fragments having different diolefin ligands (cod and nbd) between the different sites of the metallomacrocyclic framework. In fact, in addition to the species $[Rh_3(Spy)_2(cod)_2(nbd)]^+$ at m/z 837, the ESI+ mass spectrum showed the cationic fragment $[Rh_2(SpyH)(Spy)(cod)(nbd)]^+$ at m/z 627, which supports the scrambling process.

Self-Assembly Reactions Involving $[M(\mu\text{-Spy})(cod)]_2$ [M = Rh (1), Ir (2)] Metalloligands and $[M(H_2O)_2(dppp)]^{2+}$ [M = Pd (c), Pt (d)] Acceptor Units. Interestingly, our attempts to synthesize heterometallic metallomacrocycles using cis-chelated palladium(II) or platinum(II) complexes as acceptor building blocks allowed us to obtain the targeted species. As shown in Scheme 3, treatment of $[M(\mu\text{-}4\text{-}Spy)(cod)]_2$ [M = Rh (**1**), Ir (**2**)] with the square-planar compounds $[M(H_2O)_2(dppp)](OTf)_2$ [M = Pd (**c**), Pt (**d**)] in a 1:1 molar ratio in dichloromethane at room temperature allowed the preparation of the series of hexanuclear $[Rh_4Pd_2]$, $[Rh_4Pt_2]$, $[Ir_4Pd_2]$, and $[Ir_4Pt_2]$ metallocycles $(\mathbf{1c})_2$, $(\mathbf{1d})_2$, $(\mathbf{2c})_2$, and $(\mathbf{2d})_2$, respectively, which were isolated as yellow-orange solids in good yields.

Because of the presence of a diphosphine in the acceptor fragment, monitoring of the reaction solution by $^{31}P\{^1H\}$ NMR spectrometry was very helpful to confirm the formation of the targeted heteronuclear assembly in each case. After completion of the reaction (ca. 2 h), the $^{31}P\{^1H\}$ NMR spectra displayed a singlet for the palladium macrocycles $(\mathbf{1c})_2$ and $(\mathbf{2c})_2$ and a singlet, with its concomitant satellites, for the platinum species $(\mathbf{1d})_2$ and $(\mathbf{2d})_2$. The upfield shift of the ^{31}P signals together with the significant decrease in the value of the $^1J_{P-Pt}$ coupling constant evidenced the coordination of the pyridine rings to either the palladium or platinum centers.

Analogously to the $[\{M_2(\mu\text{-}4\text{-}Spy)_2(cod)_2\}_2\{M'(cod)\}_2]^{2+}$ (M, M′ = Rh, Ir) species described above, the ^{1}H NMR spectra at 298 K for the assemblies containing palladium or platinum were deceptively simple. As can be seen in Figure 6 for compound $(\mathbf{1d})_2$ as a representative example, the spectrum

Scheme 3. Self-Assembly of Hexanuclear $[M_4M'_2]$ Metallomacrocycles (M = Rh, Ir; M′ = Pd, Pt)

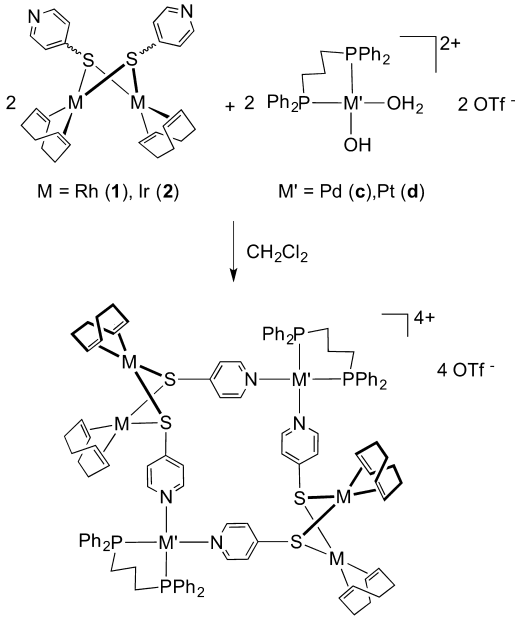

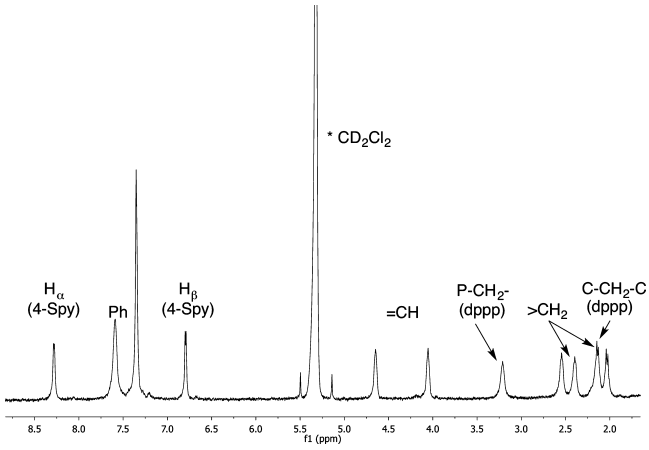

Figure 6. ^{1}H NMR spectrum (298 K, CD_2Cl_2) of the metallomacrocycle $[\{Rh_2(\mu\text{-}4\text{-}Spy)_2(cod)_2\}_2\{Pt(dppp)\}_2](OTf)_4$ $[(\mathbf{1d})_2]$.

displayed only one signal each for the α and β protons of the pyridine groups and two broad resonances (8H each) for the =CH protons of the cod ligands. The observed pattern is indicative of fluxional behavior similar to that described for the rhodium and iridium metallomacrocycles. However, in this particular case, the spectra registered in CD_2Cl_2 down to 208 K showed a large number of resonances that could not be safely interpreted.

The formation of $[\{M_2(\mu\text{-}4\text{-}Spy)_2(cod)_2\}_2\{M'(dppp)\}_2](OTf)_4$ supramolecules was further supported by high-resolution ESI+ mass spectrometry. The acetone mass spectra of the compounds showed peaks due to successive loss of triflate anions, in contrast with the assemblies described above, where the hexanuclear metallomacrocycles remained intact. For

dx.doi.org/10.1021/ic402838y | Inorg. Chem. 2014, 53, 1699−1711

example, the mass spectrum of the compound $[\{Ir_2(\mu\text{-4-Spy})_2(cod)_2\}_2\{Pd(dppp)\}_2](OTf)_4$ $[(\mathbf{2c})_2]$ (Figure 7) displays

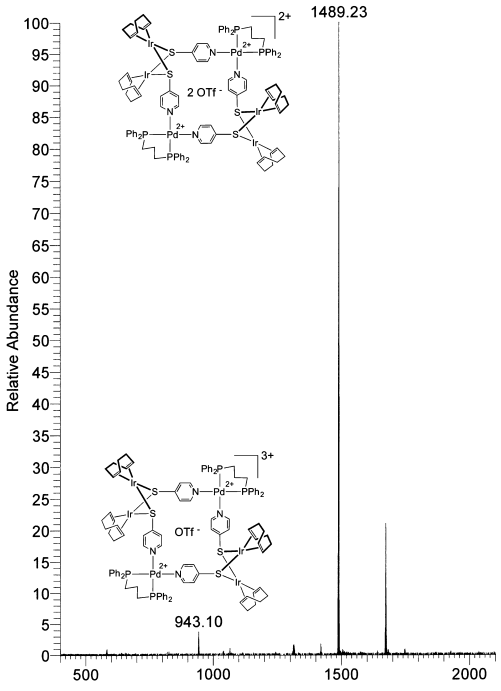

Figure 7. ESI-MS spectrum of $[\{Ir_2(\mu\text{-4-Spy})_2(cod)_2\}_2\{Pd(dppp)\}_2](OTf)_4$ $[(\mathbf{2c})_2]$.

peaks at m/z 1489.2 and 943.1 that correspond to $[(\mathbf{2c})_2 - 2OTf]^{2+}$ and $[(\mathbf{2c})_2 - 3OTf]^{3+}$, respectively. The doubly charged fragment $[(\mathbf{2c})_2 - 2OTf]^{2+}$ (Figure 7) and its analogues with $(\mathbf{1c})_2$, $(\mathbf{1d})_2$, and $(\mathbf{2d})_2$ (Figures S8–S10 in the Supporting Information) gave rise to the most intense signals, and no superimposition of smaller species with the same value of m/z was observed after the analysis of the isotope patterns. In addition, it is worth pointing out that the satisfactory mass spectra of the iridium metallomacrocycles $(\mathbf{2c})_2$ and $(\mathbf{2d})_2$ confirm the dinuclear formulation of the iridium metalloligand $[Ir(\mu\text{-4-Spy})(cod)]_2$ (**2**), whose limited solubility had precluded a complete characterization.

Furthermore, the characterization of this family of compounds was complemented with an X-ray diffraction study of a single crystal of $(\mathbf{1d})_2$ grown by slow diffusion of diethyl ether into a dichloromethane solution of the compound at 253 K. As featured in Figure 8, the crystal structure shows a square-shaped macrocyclic assembly containing $[Rh(\mu\text{-4-Spy})(cod)]_2$ binuclear ligands and Pt(dppp) groups located at alternating corners of the cationic hexametallic unit. The whole molecule resembles the molecular structure observed for $(\mathbf{1a})_2$, where the two "Rh(cod)" corners in $(\mathbf{1a})_2$ have been substituted by the "Pt(dppp)" groups (Figure S7 in the Supporting Information). The asymmetric unit of $(\mathbf{1a})_2$ contains half of the molecule, which can be expanded via the inversion symmetry operation.

An analysis of the geometrical parameters of the binuclear ligand revealed interatomic bond distances and angles (summarized in Table 3), a dihedral angle between the mean rhodium coordination planes [74.01(11)°], and a Rh···Rh interatomic distance [2.9871(8) Å] very similar to those previously observed in $(\mathbf{1a})_2$. This fact points out the potential

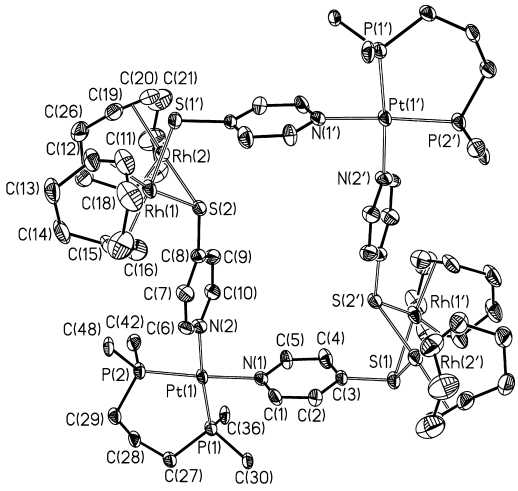

Figure 8. Molecular structure of the cation of $(\mathbf{1d})_2$. For clarity, only the ipso carbon atoms of the phenyl groups are represented. Primed atoms are related to the nonprimed ones through the symmetry operation $1 - x, -y, -z$.

Table 3. Selected Bond Lengths and Angles for $(\mathbf{1d})_2$[a]

Bond Lengths (Å)			
Rh(1)–S(1′)	2.3707(17)	Rh(2)–S(1′)	2.3474(16)
Rh(1)–S(2)	2.3781(14)	Rh(2)–S(2)	2.3688(17)
Rh(1)–G(1)	2.018(6)	Rh(2)–G(3)	2.013(7)
Rh(1)–G(2)	2.030(7)	Rh(2)–G(4)	2.027(7)
Pt(1)–P(1)	2.2631(14)	Pt(1)–N(1)	2.088(4)
Pt(1)–P(2)	2.2628(15)	Pt(1)–N(2)	2.109(4)
Bond Angles (deg)			
S(1′)–Rh(1)–S(2)	79.52(5)	S(1′)–Rh(2)–S(2)	80.18(5)
S(1′)–Rh(1)–G(1)	90.9(2)	S(1′)–Rh(2)–G(3)	90.1(2)
S(1′)–Rh(1)–G(2)	175.8(2)	S(1′)–Rh(2)–G(4)	169.7(2)
S(2)–Rh(1)–G(1)	170.3(2)	S(2)–Rh(2)–G(3)	170.2(2)
S(2)–Rh(1)–G(2)	102.3(2)	S(2)–Rh(2)–G(4)	101.7(2)
G(1)–Rh(1)–G(2)	87.3(3)	G(3)–Rh(2)–G(4)	87.5(3)
P(1)–Pt(1)–P(2)	93.22(5)	P(2)–Pt(1)–N(1)	176.82(13)
P(1)–Pt(1)–N(1)	89.46(12)	P(2)–Pt(1)–N(2)	91.92(13)
P(1)–Pt(1)–N(2)	174.85(13)	N(1)–Pt(1)–N(2)	85.40(17)

[a]G(1), G(2), G(3), and G(4) represent the centroids of the C(11)–C(12), C(15)–C(16), C(19)–C(20), and C(23)–C(24) olefinic bonds, respectively.

ability of this nonsymmetric bimetallic unit as a rigid building block to control self-assembly.

In fact, coordination of two "Pt(dppp)" fragments through the nitrogen atoms of the 4-Spy moieties gives rise to a heterometallomacrocycle with alternating Rh_2 and Pt corners. The observed Pt–N bond lengths agree with those reported for the related complexes $[(4,4'\text{-bipyridyl})_4\{Pt(dppp)\}_4](OTf)_8$,[70] $[(dipyridyldibenzotetraaza[14]annulene)_2\{Pt(dppp)\}_2](OTf)_4$,[92] $[\mathbf{L1}_4\{Pt(dppp)\}_4](OTf)_8$ [**L1** = 2-(3′-(1-methoxycarbonylethylcarbamoyl)-(4,4′)-bipyridinyl-3-carbonyl)-aminopropionic acid methyl ester],[83] $[(N,N'\text{-bis}(3,5\text{-dimethyl-4-pyridinyl})\text{-4-ethoxy-2,6-pyridinedicarboxamide})_2\{Pt(dppp)\}_2](OTf)_4$,[93] $[\mathbf{L2}_2\{Pt(dppp)\}_2](OTf)_4$ [**L2** = bis(μ_2-3,11-dimethyl-5,13-bis((pyridin-4-yl)-1,9-diazatetracyclo[7.7.1.0^{2,7}.0^{10,15}]heptadeca-2,4,6,10,12,14-hexene],[94] and $[\{Pd(\eta^3\text{-2-Me-}C_3H_4)(PPh_2py)_2\}_2\{Pt(dppp)\}_2](OTf)_6$.[31] The

dx.doi.org/10.1021/ic402838y | Inorg. Chem. 2014, 53, 1699–1711

square-planar configuration of the platinum atoms is achieved by the coordination of two nitrogen atoms of pyridine-4-thiolate units and the phosphorus atoms of a chelating dppp ligand, with P(1)−Pt(1)−N(2) and P(2)−Pt(1)−N(2) angles of 89.46(12) and 91.92(13)°, respectively, which are very close to the ideal cis angle value of 90°. Substitution of cod with dppp seems to hardly affect to the macrocyclic core dimensions, which are 6.6354(16) Å × 9.6200(15) Å for this compound.

On the other hand, the bite angle of the bidentate chelate dppp is close to those reported in the literature for M(dppp) fragments. The six-membered Pt(1)−P(1)−C(27)−C(28)−C(29)−P(2) metallocycle adopts a $^1C_4$ chair conformation [Q = 0.640(5) Å, Θ = 13.8(4)°, φ = −173(2)°].[95] Within this arrangement, $\pi\cdots\pi$ interactions between the equatorial phenyl rings of the diphosphine and the pyridine rings are observed (Figure 9 and Table S1 in the Supporting Information).

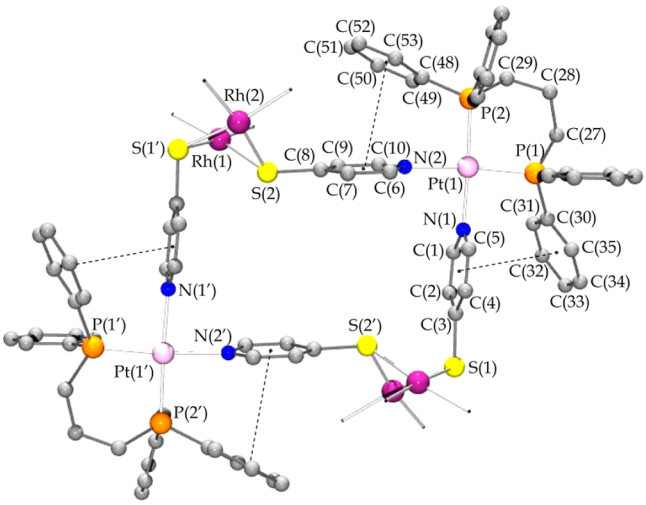

Figure 9. Schematic representation of the $\pi\cdots\pi$ interactions in $(\mathbf{1d})_2$. For clarity, carbon atoms of the cod fragments have been omitted. Primed atoms are related to the nonprimed ones through the symmetry operation $1-x, -y, -z$.

The packing arrangement of $(\mathbf{1d})_2$ is very different than that observed in $(\mathbf{1a})_2$, as it shows columnar stacking along the a axis with perfect overlay of the metallomacrocycles (Figure 10).

Self-Assembly Reactions Involving [Rh(μ-4-Spy)(nbd)]$_2$ (3) and [Rh(μ-4-Spy)(CO)(PPh$_3$)]$_2$ (4). In contrast with [Rh(μ-4-Spy)(cod)]$_2$, the dinuclear compound [Rh(μ-4-Spy)(nbd)]$_2$ (**3**) was not an effective building block. Monitoring of the reaction of **3** with [Rh(nbd)(NCCH$_3$)$_2$]$^+$ in CD_2Cl_2 evidenced the formation of the metallomacrocycle [{Rh$_2$(μ-4-Spy)$_2$(nbd)$_2$}$_2${Rh(nbd)}$_2$]$^{2+}$ which was identified by the set of characteristic resonances for the α and β protons of the pyridine-4-thiolato ligands: four doublets at 8.22, 8.18, 7.08, and 6.90 ppm ($^1J_{H-H} \approx 6$ Hz). However, we could not isolate a well-defined product in the solid state, and after several attempts, we were able to obtain only orange solids with poorly defined NMR spectra. Most probably, this fact could be a consequence of the lability of the formed assembly, which is in agreement with the stronger π-acceptor character of the 2,5-norbornadiene ligands compared with 1,5-cyclooctadiene, which in turn reduces the electron density on the peripheral nitrogen donor atoms, thereby decreasing their coordinating ability.

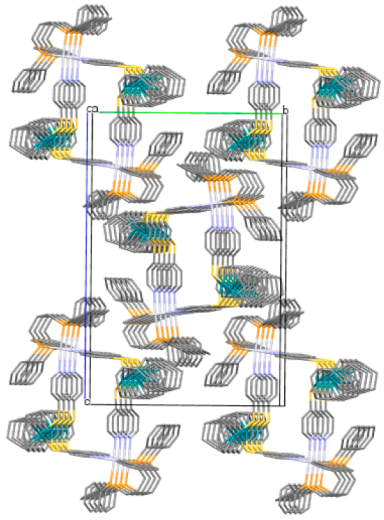

Figure 10. Packing diagram for $(\mathbf{1d})_2$. For simplicity, hydrogen atoms, counterions, and solvent molecules have been omitted.

A potential catalytic application of the diolefin-based metallomacrocycles is olefin hydroformylation.[47,96] However, under syngas (H_2/CO) pressure and an excess of phosphine ligand, the diolefin rhodium catalyst precursors are readily transformed into the corresponding CO/PPh$_3$ derivatives. In order to explore the stability of the metallocycles based on "Rh(CO)(PPh$_3$)" metal fragments, self-assembly reactions involving the metalloligand [Rh(μ-4-Spy)(CO)(PPh$_3$)]$_2$ (**4**) were carried out. The reaction of **4** with [Rh(cod)(NCCH$_3$)$_2$]-BF$_4$ (**a**) in a 1:1 molar ratio in CH_2Cl_2 gave an orange-brown crude product that was isolated after the addition of diethyl ether. Interestingly, in contrast to what was observed for the previously described metallomacrocycles, the NMR spectra of this material indicated the presence of a mixture of self-assembled species with a clear predominance of one of them. Thus, the ^{1}H NMR spectrum (Figure S11 in the Supporting Information) showed four intense sharp doublets that indicated the equivalence of pyridines into pairs, while the ^{31}P{^{1}H} NMR spectrum (Figure S12 in the Supporting Information) displayed as the most intense resonance a doublet ($^1J_{P-Rh}$ = 129 Hz), in accordance with the equivalence of the four phosphorus nuclei. In addition, the ^{1}H−^{1}H NOESY spectrum showed proximity cross-peaks between one of the pyridine β-protons and a phenyl group of triphenylphosphine. Since metalloligand **4** can adopt different structures depending on the relative disposition of the PPh$_3$ and CO ligands, four different isomeric metallocycles can be envisaged, including two cis−cis ones (C_{2h} and C_s symmetry) and two trans−trans ones (C_1 and C_2 symmetry). The NMR data strongly suggest that the major species from the **4** + **a** self-assembly should be the cis−cis isomer with C_{2h} symmetry (represented in Figure 11), which reinforces the proposed cis disposition of the PPh$_3$/CO ligands in compound **4**.

CONCLUSIONS

The dinuclear complexes [M(4-Spy)(cod)]$_2$ (M = Rh, Ir) supported by bridging pyridine-4-thiolato ligands have been proved to be effective ditopic building blocks for the construction of new supramolecular architectures. The two nucleophilic nitrogen atoms of the terminal pyridine groups allow these compounds to self-assemble with suitable acceptor

dx.doi.org/10.1021/ic402838y | Inorg. Chem. 2014, 53, 1699−1711

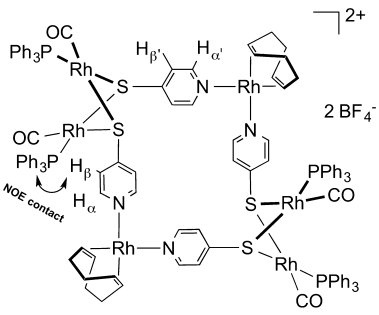

Figure 11. Proposed structure of the predominant species from the self-assembly of $[Rh(\mu\text{-}4\text{-Spy})(CO)(PPh_3)]_2$ (**4**) and $[Rh(cod)(NCCH_3)_2]BF_4$ (**a**).

metallic fragments $[M(cod)(NCCH_3)_2]^+$ (M = Rh, Ir) or $[M(H_2O)_2(dppp)](OTf)_2$ (M = Pd, Pt), yielding hexanuclear homo- and heterometallomacrocycles of composition $[Rh_4M_2]$ and $[Ir_4M_2]$. These supramolecular species are composed of alternating dinuclear (Rh_2 or Ir_2) and mononuclear corners (Rh, Ir, Pd, or Pt) supported by four bridging pyridine-4-thiolate linkers, resulting in rectangular assemblies with cavities of 9.6 Å × 6.6 Å.

Although multinuclear NMR spectroscopy is indicative of a syn disposition of the pyridine-4-thiolate fragments in the free dinuclear metalloligands, the anti conformation adopted by these compounds when forming the metallocycles implies a process of sulfur inversion associated with the self-assembly reactions. In addition, all of the obtained macrocycles are stereochemically nonrigid in solution. The study of this behavior by ^1H NMR spectroscopy revealed the existence of a dynamic equilibrium between the supramolecular species and their corresponding building blocks.

The related dinuclear complexes $[Rh(4\text{-Spy})(nbd)]_2$ and $[Rh(4\text{-Spy})(CO)(PPh_3)]_2$ did not self-assemble as effectively as $[M(4\text{-Spy})(cod)]_2$ (M = Rh, Ir). The metallomacrocycles involving $[Rh(4\text{-Spy})(nbd)]_2$ were found to be labile, which precluded their isolation from the reaction solution. This fact could be related to the stronger π-acceptor character of ndb compared to cod, which reduces the coordination ability of the pyridine fragments. On the other hand, the complex $[Rh(4\text{-Spy})(CO)(PPh_3)]_2$ gave a mixture of supramolecules derived from the relative disposition of the CO and PPh_3 ligands at the rhodium centers.

Finally, the introduction of Rh(cod) functionality in these supramolecules opens the possibility of future studies of their catalytic activities in several processes.

■ ASSOCIATED CONTENT

Ⓢ Supporting Information

X-ray crystallographic files in CIF format for the structure determination of metallomacrocycles $(\mathbf{1a})_2$ and $(\mathbf{1d})_2$; NMR spectra of $(\mathbf{1a})_2$ and $(\mathbf{4a})_2$; ESI-MS spectra of $(\mathbf{1c})_2$, $(\mathbf{1d})_2$, and $(\mathbf{2d})_2$; and geometrical parameters of the $\pi\cdots\pi$ interactions in $(\mathbf{1d})_2$. This material is available free of charge via the Internet at http://pubs.acs.org.

■ AUTHOR INFORMATION

Corresponding Authors

*E-mail: montse.ferrer@qi.ub.es (M.F.).
*E-mail: perez@unizar.es (J.J.P.-T.).

Notes

The authors declare no competing financial interest.

■ ACKNOWLEDGMENTS

Financial support for this work was provided by the Ministerio de Economía y Competitividad (MINECO/FEDER) of Spain (Projects CTQ2010-15221 and CTQ2012-31335), Diputación General de Aragón (Group E07), and Fondo Social Europeo.

■ REFERENCES

(1) Leininger, S.; Olenyuk, B.; Stang, P. J. *Chem. Rev.* **2000**, *100*, 853−907.
(2) Swiegers, G. F.; Malefetse, T. J. *Chem. Rev.* **2000**, *100*, 3483−3537.
(3) Cotton, F. A.; Lin, C.; Murillo, C. A. *Acc. Chem. Res.* **2001**, *34*, 759−771.
(4) Cronin, L. *Annu. Rep. Prog. Chem., Sect. A: Inorg. Chem.* **2004**, *100*, 323−383.
(5) Wurthner, F.; You, C. C.; Saha-Moller, C. R. *Chem. Soc. Rev.* **2004**, *33*, 133−146.
(6) Amijs, C. H. M.; van Klink, G. P. M.; van Koten, G. *Dalton Trans.* **2006**, 308−327.
(7) Chen, C. L.; Zhang, J. Y.; Su, C. Y. *Eur. J. Inorg. Chem.* **2007**, 2997−3010.
(8) Nitschke, J. R. *Acc. Chem. Res.* **2007**, *40*, 103−112.
(9) Kumar, A.; Sun, S. S.; Lees, A. J. *Coord. Chem. Rev.* **2008**, *252*, 922−939.
(10) Northrop, B. H.; Yang, H. B.; Stang, P. J. *Chem. Commun.* **2008**, 5896−5908.
(11) Northrop, B. H.; Zheng, Y. R.; Chi, K. W.; Stang, P. J. *Acc. Chem. Res.* **2009**, *42*, 1554−1563.
(12) Chakrabarty, R.; Mukherjee, P. S.; Stang, P. J. *Chem. Rev.* **2011**, *111*, 6810−6918.
(13) Amouri, H.; Desmarets, C.; Moussa, J. *Chem. Rev.* **2012**, *112*, 2015−2041.
(14) Cook, T. R.; Zheng, Y. R.; Stang, P. J. *Chem. Rev.* **2013**, *113*, 734−777.
(15) Pariya, C.; Sparrow, C. R.; Back, C. K.; Sandi, G.; Fronczek, F. R.; Maverick, A. W. *Angew. Chem., Int. Ed.* **2007**, *46*, 6305−6308.
(16) Chatterjee, B.; Noveron, J. C.; Resendiz, M. J. E.; Liu, J.; Yamamoto, T.; Parker, D.; Cinke, M.; Nguyen, C. V.; Arif, A. M.; Stang, P. J. *J. Am. Chem. Soc.* **2004**, *126*, 10645−10656.
(17) Yoshizawa, M.; Klosterman, J. K.; Fujita, M. *Angew. Chem., Int. Ed.* **2009**, *48*, 3418−3438.
(18) Lee, S. J.; Lin, W. B. *Acc. Chem. Res.* **2008**, *41*, 521−537.
(19) Zhang, Q. A.; He, L. S.; Liu, J. M.; Wang, W.; Zhang, J. Y.; Su, C. Y. *Dalton Trans.* **2010**, *39*, 11171−11179.
(20) Milde, B.; Packheiser, R.; Hildebrandt, S.; Schaarschmidt, D.; Ruffer, T.; Lang, H. *Organometallics* **2012**, *31*, 3661−3671.
(21) Schelter, E. J.; Prosvirin, A. V.; Dunbar, K. R. *J. Am. Chem. Soc.* **2004**, *126*, 15004−15005.
(22) Karadas, F.; Schelter, E. J.; Prosvirin, A. V.; Bacsa, J.; Dunbar, K. R. *Chem. Commun.* **2005**, 1414−1416.
(23) Ono, K.; Yoshizawa, M.; Tatsuhisa, K. C.; Fujita, M. *Chem. Commun.* **2008**, 2328−2330.
(24) Han, F. S.; Higuchi, M.; Kurth, D. G. *J. Am. Chem. Soc.* **2008**, *130*, 2073−2081.
(25) Sun, Q. F.; Wong, K. M. C.; Liu, L. X.; Huang, H. P.; Yu, S. Y.; Yam, V. W. W.; Li, Y. Z.; Pan, Y. J.; Yu, K. C. *Inorg. Chem.* **2008**, *47*, 2142−2154.
(26) Yamamoto, Y.; Tamaki, Y.; Yui, T.; Koike, K.; Ishitani, O. *J. Am. Chem. Soc.* **2010**, *132*, 11743−11752.
(27) Steed, J. W. *Chem. Soc. Rev.* **2009**, *38*, 506−519.
(28) Gao, J.; Riis-Johannessen, T.; Scopelliti, R.; Qian, X. H.; Severin, K. *Dalton Trans.* **2010**, *39*, 7114−7118.
(29) Yao, L. Y.; Qin, L.; Xie, T. Z.; Li, Y. Z.; Yu, S. Y. *Inorg. Chem.* **2011**, *50*, 6055−6062.
(30) Alvarez-Vergara, M. C.; Casado, M. A.; Martin, M. L.; Lahoz, F. J.; Oro, L. A.; Perez-Torrente, J. J. *Organometallics* **2005**, *24*, 5929−5936.

(31) Angurell, I.; Ferrer, M.; Gutierrez, A.; Martinez, M.; Rodriguez, L.; Rossell, O.; Engeser, M. *Chem.—Eur. J.* **2010**, *16*, 13960−13964.
(32) Ferrer, M.; Gutierrez, A.; Rodriguez, L.; Rossell, O.; Ruiz, E.; Engeser, M.; Lorenz, Y.; Schilling, R.; Gomez-Sal, P.; Martin, A. *Organometallics* **2012**, *31*, 1533−1545.
(33) Zanardi, A.; Mata, J. A.; Peris, E. *J. Am. Chem. Soc.* **2009**, *131*, 14531−14537.
(34) Suijkerbuijk, B. M. J. M.; Schamhart, D. J.; Kooijman, H.; Spek, A. L.; van Koten, G.; Gebbink, R. J. M. K. *Dalton Trans.* **2010**, *39*, 6198−6216.
(35) Park, J.; Hong, S. *Chem. Soc. Rev.* **2012**, *41*, 6931−6943.
(36) Bera, J. K.; Smucker, B. W.; Walton, R. A.; Dunbar, K. R. *Chem. Commun.* **2001**, 2562−2563.
(37) Bera, J. K.; Bacsa, J.; Smucker, B. W.; Dunbar, K. R. *Eur. J. Inorg. Chem.* **2004**, 368−375.
(38) Kuang, S. M.; Fanwick, P. E.; Walton, R. A. *Inorg. Chem.* **2002**, *41*, 1036−1038.
(39) Song, L. C.; Jin, G. X.; Zhang, W. X.; Hu, Q. M. *Organometallics* **2005**, *24*, 700−706.
(40) Cotton, F. A.; Jin, J. Y.; Li, Z.; Liu, C. Y.; Murillo, C. A. *Dalton Trans.* **2007**, 2328−2335.
(41) Zhao, L.; Ghosh, K.; Zheng, Y.; Lyndon, M. M.; Williams, T. I.; Stang, P. J. *Inorg. Chem.* **2009**, *48*, 5590−5592.
(42) Ara, I.; Chaouche, N.; Fornies, J.; Fortuno, C.; Kribii, A.; Martin, A. *Eur. J. Inorg. Chem.* **2005**, 3894−3901.
(43) Ciriano, M. A.; Perez-Torrente, J. J.; Lahoz, F. J.; Oro, L. A. *J. Chem. Soc., Dalton Trans.* **1992**, 1831−1837.
(44) Casado, M. A.; Perez-Torrente, J. J.; Lopez, J. A.; Ciriano, M. A.; Lahoz, F. J.; Oro, L. A. *Inorg. Chem.* **1999**, *38*, 2482−2488.
(45) Miranda-Soto, V.; Perez-Torrente, J. J.; Oro, L. A.; Lahoz, F. J.; Martin, M. L.; Parra-Hake, M.; Grotjahn, D. B. *Organometallics* **2006**, *25*, 4374−4390.
(46) Hernandez-Gruel, M. A. F.; Gracia-Arruego, G.; Rivas, A. B.; Dobrinovitch, I. T.; Lahoz, F. J.; Pardey, A. J.; Oro, L. A.; Perez-Torrente, J. J. *Eur. J. Inorg. Chem.* **2007**, 5677−5683.
(47) Rivas, A. B.; Gascon, J.; Lahoz, F. J.; Balana, A. I.; Pardey, A. J.; Oro, L. A.; Perez-Torrente, J. J. *Inorg. Chem.* **2008**, *47*, 6090−6104.
(48) Perez-Torrente, J. J.; Jimenez, M. V.; Hernandez-Gruel, M. A. E.; Fabra, M. J.; Lahoz, F. J.; Oro, L. A. *Chem.—Eur. J.* **2009**, *15*, 12212−12222.
(49) Aullon, G.; Ujaque, G.; Lledos, A.; Alvarez, S. *Chem.—Eur. J.* **1999**, *5*, 1391−1410.
(50) Capdevila, M.; Gonzalez-Duarte, P.; Foces-Foces, C.; Cano, F. H.; Martinez-Ripoll, M. *J. Chem. Soc., Dalton Trans.* **1990**, 143−149.
(51) Rivera, G.; Bernes, S.; de Barbarin, C.; Torrens, H. *Inorg. Chem.* **2001**, *40*, 5575−5580.
(52) Oster, S. S.; Jones, W. D. *Inorg. Chim. Acta* **2004**, *357*, 1836−1846.
(53) Chikamoto, Y.; Kawamoto, T.; Igashira-Kamiyama, A.; Konno, T. *Inorg. Chem.* **2005**, *44*, 1601−1610.
(54) Chong, S. H.; Koh, L. L.; Henderson, W.; Hor, T. S. A. *Chem.—Asian J.* **2006**, *1*, 264−272.
(55) Boudreau, J.; Grenier-Desbiens, J.; Fontaine, F. G. *Eur. J. Inorg. Chem.* **2010**, 2158−2164.
(56) Ruiz, N.; Castillon, S.; Ruiz, A.; Claver, C.; Aaliti, A.; Alvarez-Larena, A.; Piniella, J. F.; Germain, G. *J. Chem. Soc., Dalton Trans.* **1996**, 969−973.
(57) Castellanos-Paez, A.; Thayaparan, J.; Castillon, S.; Claver, C. *J. Organomet. Chem.* **1998**, *551*, 375−381.
(58) Bayon, J. C.; Claver, C.; Masdeu-Bulto, A. M. *Coord. Chem. Rev.* **1999**, *193*−*195*, 73−145.
(59) Pamies, O.; Net, G.; Ruiz, A.; Bo, C.; Poblet, J. M.; Claver, C. *J. Organomet. Chem.* **1999**, *586*, 125−137.
(60) Freixa, Z.; Martin, E.; Gladiali, S.; Bayon, J. C. *Appl. Organomet. Chem.* **2000**, *14*, 57−65.
(61) Han, Y. F.; Lin, Y. J.; Jia, W. G.; Jin, G. X. *Dalton Trans.* **2009**, 2077−2080.
(62) Wang, H.; Guo, X. Q.; Zhong, R.; Lin, Y. J.; Zhang, P. C.; Hou, X. F. *J. Organomet. Chem.* **2009**, *694*, 3362−3368.
(63) Wang, H.; Zhong, R.; Guo, X. Q.; Feng, X. Y.; Hou, X. F. *Eur. J. Inorg. Chem.* **2010**, 174−178.
(64) Tzeng, B. C.; Ding, C. S.; Chang, T. Y.; Hu, C. C.; Lee, G. H. *CrystEngComm* **2012**, *14*, 8228−8235.
(65) Giordano, G.; Crabtree, R. H. *Inorg. Synth.* **1979**, *19*, 218−220.
(66) Abel, E. W.; Bennett, M. A.; Wilkinson, G. *J. Chem. Soc.* **1959**, 3178−3182.
(67) Herde, J. L.; Lambert, J. C.; Senoff, C. V. *Inorg. Synth.* **1971**, *15*, 18−20.
(68) Uson, R.; Oro, L. A.; Cabeza, J. A.; Bryndza, H. E.; Stepro, M. P. *Inorg. Synth.* **1985**, *23*, 126−127.
(69) Jegorov, A.; Podlaha, J.; Podlahova, J.; Turecek, F. *J. Chem. Soc., Dalton Trans.* **1990**, 3259−3263.
(70) Stang, P. J.; Cao, D. H.; Saito, S.; Arif, A. M. *J. Am. Chem. Soc.* **1995**, *117*, 6273−6283.
(71) Green, M.; Kuc, T. A.; Taylor, S. H. *J. Chem. Soc. A* **1971**, 2334−2335.
(72) *SAINT-PLUS: Area Detector Integration Software*, version 6.01; Bruker AXS: Madison, WI, 2001.
(73) *SADABS: Area Detector Absorption Correction Program*; Bruker AXS: Madison, WI, 1996.
(74) Sheldrick, G. M. *Acta Crystallogr.* **1990**, *A46*, 467−473.
(75) Sheldrick, G. M. *Methods Enzymol.* **1997**, *276*, 628−641.
(76) Sheldrick, G. M. *Acta Crystallogr.* **2008**, *A64*, 112−122.
(77) Nardelli, M. *Comput. Chem.* **1983**, *7*, 95−98.
(78) Nardelli, M. *J. Appl. Crystallogr.* **1995**, *28*, 659−673.
(79) Cotton, F. A.; Lin, C.; Murillo, C. A. *Inorg. Chem.* **2001**, *40*, 478−484.
(80) Teo, P.; Koh, L. L.; Hor, T. S. A. *Inorg. Chem.* **2008**, *47*, 6464−6474.
(81) Granzhan, A.; Riis-Johannessen, T.; Scopelliti, R.; Severin, K. *Angew. Chem., Int. Ed.* **2010**, *49*, 5515−5518.
(82) Wang, X. B.; Huang, J.; Xiang, S. L.; Liu, Y.; Zhang, J. Y.; Eichhofer, A.; Fenske, D.; Bai, S.; Su, C. Y. *Chem. Commun.* **2011**, *47*, 3849−3851.
(83) Rang, A.; Nieger, M.; Engeser, M.; Lutzen, A.; Schalley, C. A. *Chem. Commun.* **2008**, 4789−4791.
(84) Vandersluis, P.; Spek, A. L. *Acta Crystallogr.* **1990**, *A46*, 194−201.
(85) Abel, E. W.; Bhargava, S. K.; Orrell, K. G. *Prog. Inorg. Chem.* **1984**, *32*, 1−118.
(86) Brunner, H.; Bugler, J.; Nuber, B. *Tetrahedron: Asymmetry* **1996**, *7*, 3095−3098.
(87) Fernandez, E.; Ruiz, A.; Castillon, S.; Claver, C.; Piniella, J. F.; Alvarez-Larena, A.; Germain, G. *J. Chem. Soc., Dalton Trans.* **1995**, 2137−2142.
(88) Fandos, R.; Martinez-Ripoll, M.; Otero, A.; Ruiz, M. J.; Rodriguez, A.; Terreros, P. *Organometallics* **1998**, *17*, 1465−1470.
(89) Wark, T. A.; Stephan, D. W. *Can. J. Chem.* **1990**, *68*, 565−569.
(90) Jones, W. D.; Garcia, J.; Torrens, H. *Acta Crystallogr.* **2005**, *E61*, M2204−M2206.
(91) Delferro, M.; Cauzzi, D.; Pattacini, R.; Tegoni, M.; Graiff, C.; Tiripicchio, A. *Eur. J. Inorg. Chem.* **2008**, 2302−2312.
(92) Beves, J. E.; Chapman, B. E.; Kuchel, P. W.; Lindoy, L. F.; McMurtrie, J.; McPartlin, M.; Thordarson, P.; Wei, G. *Dalton Trans.* **2006**, 744−750.
(93) Capo, M.; Benet-Buchholz, J.; Ballester, P. *Inorg. Chem.* **2008**, *47*, 10190−10192.
(94) Weilandt, T.; Kiehne, U.; Bunzen, J.; Schnakenburg, G.; Lutzen, A. *Chem.—Eur. J.* **2010**, *16*, 2418−2426.
(95) Cremer, D.; Pople, J. A. *J. Am. Chem. Soc.* **1975**, *97*, 1354−1358.
(96) Leighton, J. L. *Modern Rhodium-Catalyzed Organic Reactions*; Wiley-VCH: Weinheim, Germany, 2005.